

NAVAL POSTGRADUATE SCHOOL

Monterey, California



THESIS

SPACECRAFT POWER BEAMING AND SOLAR CELL ANNEALING USING HIGH-ENERGY LASERS

by

Richard C. Luce, Jr.

December 2002

Thesis Advisor:
Co-Advisor:

Sherif Michael
Oscar Biblarz

Approved for public release; distribution is unlimited

THIS PAGE INTENTIONALLY LEFT BLANK

REPORT DOCUMENTATION PAGE			<i>Form Approved OMB No. 0704-0188</i>	
Public reporting burden for this collection of information is estimated to average 1 hour per response, including the time for reviewing instruction, searching existing data sources, gathering and maintaining the data needed, and completing and reviewing the collection of information. Send comments regarding this burden estimate or any other aspect of this collection of information, including suggestions for reducing this burden, to Washington headquarters Services, Directorate for Information Operations and Reports, 1215 Jefferson Davis Highway, Suite 1204, Arlington, VA 22202-4302, and to the Office of Management and Budget, Paperwork Reduction Project (0704-0188) Washington DC 20503.				
1. AGENCY USE ONLY (Leave blank)		2. REPORT DATE December 2002	3. REPORT TYPE AND DATES COVERED Master's Thesis	
4. TITLE AND SUBTITLE: Spacecraft Power Beaming and Solar Cell Annealing Using High-Energy Lasers			5. FUNDING NUMBERS	
6. AUTHOR(S) Luce, Richard C. Jr.				
7. PERFORMING ORGANIZATION NAME(S) AND ADDRESS(ES) Naval Postgraduate School Monterey, CA 93943-5000			8. PERFORMING ORGANIZATION REPORT NUMBER	
9. SPONSORING /MONITORING AGENCY NAME(S) AND ADDRESS(ES) N/A			10. SPONSORING/MONITORING AGENCY REPORT NUMBER	
11. SUPPLEMENTARY NOTES: The views expressed in this thesis are those of the author and do not reflect the official policy or position of the Department of Defense or the U.S. Government.				
12a. DISTRIBUTION / AVAILABILITY STATEMENT Approved for public release; distribution unlimited.			12b. DISTRIBUTION CODE A	
13. ABSTRACT (maximum 200 words) Satellite lifetime is often limited by degradation of the electrical power subsystem--radiation-damaged solar arrays and failed batteries. Being able to beam power from terrestrial sites could alleviate this limitation, extending the lifetime of billions of dollars of satellite assets, as well as providing additional energy for electric propulsion that can be used for stationkeeping and orbital changes. In addition, laboratory research at the Naval Postgraduate School (NPS) has shown the potential to anneal damaged solar cells using lasers. This thesis describes that research, preliminary work performed lasing a representative solar panel array, and a proposed Maui experiment to demonstrate the relevant concepts by lasing PANSAT, an NPS-built and operated spacecraft. The preliminary work done at Maui involved lasing a PANSAT silicon photovoltaic array using a 975 nm Yb:YAG source at output power levels of 7 W, 14 W and 21 W. These results matched those obtained under near-AM0 conditions atop Mount Haleakala (for the 7 W case) and extrapolated to match predicted output levels. Enough data points were collected at each power level to generate an I-V curve for the panel, identifying the open circuit voltage, short circuit current, and maximum power points. The efficiency of the panel varied from 13.1% (as expected for monochromatic light) at 7 W to 11.3% at 21 W due to uniform heating of the cells. These results represent a "ground truth" baseline from which further research can continue.				
14. SUBJECT TERMS Laser, solar cell, photovoltaics, power beaming, annealing, wireless power transmission, electric propulsion, PANSAT			15. NUMBER OF PAGES 95	
			16. PRICE CODE	
17. SECURITY CLASSIFICATION OF REPORT Unclassified	18. SECURITY CLASSIFICATION OF THIS PAGE Unclassified	19. SECURITY CLASSIFICATION OF ABSTRACT Unclassified	20. LIMITATION OF ABSTRACT UL	

THIS PAGE INTENTIONALLY LEFT BLANK

Approved for public release; distribution unlimited

**SPACECRAFT POWER BEAMING AND SOLAR CELL ANNEALING USING
HIGH-ENERGY LASERS**

Richard C. Luce, Jr.
Captain, United States Air Force
M.S., University of Central Florida, 1999

Submitted in partial fulfillment of the
requirements for the degree of

MASTER OF SCIENCE IN ASTRONAUTICAL ENGINEERING

from the

**NAVAL POSTGRADUATE SCHOOL
December 2002**

Author: Richard C. Luce, Jr.

Approved by: Sherif Michael
Thesis Advisor

Oscar Biblarz
Co-Advisor

Max Platzer
Chairman, Department of Aeronautics and Astronautics

THIS PAGE INTENTIONALLY LEFT BLANK

ABSTRACT

Satellite lifetime is often limited by degradation of the electrical power subsystem--radiation-damaged solar arrays and failed batteries. Being able to beam power from terrestrial sites could alleviate this limitation, extending the lifetime of billions of dollars of satellite assets, as well as providing additional energy for electric propulsion that can be used for stationkeeping and orbital changes. In addition, laboratory research at the Naval Postgraduate School (NPS) has shown the potential to anneal damaged solar cells using lasers. This thesis describes that research, preliminary work performed lasing a representative solar panel array, and a proposed on-orbit experiment to demonstrate the relevant concepts by lasing PANSAT, an NPS-built and operated spacecraft.

The preliminary work done at Maui involved lasing a PANSAT silicon photovoltaic array using a 975 nm Yb:YAG source at output power levels of 7 W, 14 W and 21 W. These results matched those obtained under near-AM0 conditions atop Mount Haleakala (for the 7 W case) and extrapolated to match predicted output levels. Enough data points were collected at each power level to generate an I-V curve for the panel, identifying the open circuit voltage, short circuit current, and maximum power points. The efficiency of the panel varied from 13.1% (as expected for monochromatic light) at 7 W to 11.3% at 21 W due to uniform heating of the cells. These results represent a “ground truth” baseline from which further research can continue.

THIS PAGE INTENTIONALLY LEFT BLANK

TABLE OF CONTENTS

I.	INTRODUCTION.....	1
II.	GROUND-BASED LASERS.....	3
A.	LASER CONCEPTS	3
B.	GROUND-BASED HIGH-ENERGY LASER FACILITIES	7
	1. MIT/LL Firepond Research Site	8
	2. Air Force Maui Optical and Supercomputing Site (AMOS)	11
	3. White Sands Missile Range (WSMR) High-Energy Laser Systems Test Facility (HELSTF).....	13
	4. AFRL Starfire Optical Range (SOR).....	15
	5. SELENE (Space Laser Energy).....	18
C.	CONCLUSION	19
III.	AIR- AND SPACE-BASED LASERS.....	21
A.	LIMITATIONS OF GROUND-BASED LASERS	21
B.	THE AIRBORNE LASER	24
C.	THE SPACE-BASED LASER.....	27
IV.	ELECTRIC PROPULSION	29
A.	INTRODUCTION.....	29
B.	APPLICATIONS OF ELECTRIC PROPULSION.....	31
	1. Electric Propulsion for Stationkeeping.....	31
	2. Electric Propulsion for Orbit Raising.....	33
	3. Electric Propulsion for Orbital Maneuvering.....	35
V.	PHOTOVOLTAIC CELLS	37
A.	SOLAR CELL TECHNOLOGY.....	37
	1. Silicon Solar Cells	39
	2. Gallium Arsenide Solar Cells.....	42
	3. Multijunction Solar Cells	43
B.	PHOTOVOLTAIC POWER CONVERSION OF LASER ENERGY	45
VI.	ANNEALING OF RADIATION-DAMAGED SOLAR CELLS.....	47
A.	RADIATION DAMAGE	47
B.	ANNEALING METHODS.....	48
	1. Thermal Annealing	48
	2. Current Annealing.....	49
	3. Conclusion	50
C.	MEASURING CELL OUTPUT	50
VII.	GROUND AND ON-ORBIT TESTING	55
A.	THE PETITE AMATEUR NAVY SATELLITE (PANSAT).....	55
	1. PANSAT Overview	55
	2. Suitability for On-Orbit Testing.....	59
B.	GROUND-BASED TESTING	62

C. ON-ORBIT TEST PLAN	69
VIII. CONCLUSION AND RECOMMENDATIONS	73
LIST OF REFERENCES	75
INITIAL DISTRIBUTION LIST	79

LIST OF FIGURES

Figure 2.1	Unstable Resonator Schematic (Kuhn, p. 112).....	4
Figure 2.2	Firepond Lidar in Action	8
Figure 2.3	Firepond Lidar Schematic Diagram.....	9
Figure 2.4	Spectra-Physics GCR-6 Laser at Firepond	10
Figure 2.5	Firepond 1.2 meter Telescope.....	10
Figure 2.6	AMOS Telescopes	11
Figure 2.7	LURE Telescopes	13
Figure 2.8	HELSTF Facilities	14
Figure 2.9	Inside the MIRACL Facility	15
Figure 2.10	SOR Telescopes and Mounts.....	16
Figure 2.11	Laser Beacon Propagation from the 1.5 m Telescope	17
Figure 2.12	The FEL Principle.....	19
Figure 3.1	Strehl Ratio vs Wavelength	23
Figure 3.2	Atmospheric Transmission at Sea Level.....	24
Figure 3.3	ABL Engaging a Target.....	25
Figure 3.4	ABL Schematic Diagram.....	26
Figure 3.5	SBL Engages a Target	28
Figure 4.1	Boeing XIPS Schematic Diagram.....	33
Figure 5.1	Inside a Photovoltaic Cell (image courtesy DoE).....	38
Figure 5.2	Single Crystal Solar Cells (image courtesy ACRE)	40
Figure 5.3	Polycrystalline Solar Cells (image courtesy ACRE)	41
Figure 5.4	Amorphous Solar Cells (image courtesy ACRE)	41
Figure 5.5	Multijunction Cell Materials and Solar Illumination.....	44
Figure 5.6	Trends in Air Force-Funded Space Solar Cell Development	45
Figure 6.1	Circuit for Measuring Cell Characteristics	51
Figure 6.2	Solar Cell I-V Curves (Carr).....	52
Figure 7.1	PANSAT Ground Trace (Peat)	56
Figure 7.2	PANSAT Solar Panel Identification (Sakoda).....	57
Figure 7.3	PANSAT Schematic Diagram (Sakoda).....	58
Figure 7.4	PANSAT Assembly Photo (Sakoda)	59
Figure 7.5	PANSAT and Ground-Based Laser Sites	61
Figure 7.6	Example of PANSAT Solar Panel Telemetry.....	62
Figure 7.7	Laser Used for Ground Testing.....	63
Figure 7.8	PANSAT Panel I-V Curve Under Solar Illumination.....	64
Figure 7.9	Lab Bench Setup	65
Figure 7.10	PANSAT Panel I-V Curve Under 7W Laser Illumination	66
Figure 7.11	PANSAT Panel I-V Curve Under 14W Laser Illumination	67
Figure 7.12	PANSAT Panel I-V Curve Under 21 W Laser Illumination	68

THIS PAGE INTENTIONALLY LEFT BLANK

LIST OF TABLES

Table 2.1	Common High-Energy Lasers	6
Table 2.2	Lasers Available at SOR.....	18
Table 4.1	Propulsion Systems Comparison	30
Table 7.1	PANSAT Orbital Elements.....	56
Table 7.2	Summary of PANSAT Panel Results	68
Table 7.3	Required Laser Power Levels	69

THIS PAGE INTENTIONALLY LEFT BLANK

ACKNOWLEDGMENTS

I would like first of all like to thank my wife for her unconditional love and support. Her tolerance of my long work hours, extended travel, and seemingly endless discussions on topics of little interest is amazing! Still, I'm glad I did not have to test her patience with any more research trips to Maui...

I also owe so much to my dedicated parents. They made truly remarkable sacrifices to provide me with such a solid upbringing. Their encouragement and bottomless well of love have enabled me to be successful in so many ways.

I cannot say enough good things about my thesis advisor, Professor Sherif Michael. He was willing to accept a grad student's crazy idea for performing some experiments, and then wholeheartedly supported the endeavor from start to finish. His passion for his work is exceeded only by his knowledge, and his enthusiasm is infectious.

To Josh Snodgrass and Maynard Porter at AMOS I say "Mahalo much" for their eager support of my project and for helping me get experiments done at the Maui site. They also put me in touch with Mark Henley at Boeing Phantom Works who had the vision to see how this thesis work would complement projects underway at AFRL and NASA Marshall Space Flight Center.

The danger in writing acknowledgments is that some key person is inevitably left out by mistake. I apologize for that, for there were truly countless individuals at locations all around the country who saw the value in my work and then contributed their time, knowledge, and effort. Thank you one and all!

THIS PAGE INTENTIONALLY LEFT BLANK

I. INTRODUCTION

It's amazing how little has actually changed in spacecraft design in the nearly fifty years we as a civilization have been building satellites. There is a payload that performs a specific mission and a bus that provides all the support needed to operate the payload. The bus has components such as attitude control, thermal control, propulsion, power supply and regulation. We use expensive, heavy, polluting, relatively unreliable chemical rockets to launch the satellites into orbit (although it should be pointed out that without these rockets, we would not have had access to space at all). And despite knowing exactly which spacecraft components are prone to failure over time, we are unable to mitigate these risks due to cost, volume, and weight constraints. Every advancement in satellite design has been incremental—not a single truly revolutionary technology has emerged to change the way scientists and engineers look at spacecraft design.

What if one of the most common sources of ending spacecraft lives were eliminated from future designs? What if this design change would enable satellites to stay on orbit virtually indefinitely, performing their missions much, much longer than currently planned? How much money would it save the government and private industry not to have to replace otherwise perfectly healthy spacecraft when this one supporting subsystem was no longer a leading cause of failure? How much more effort could we put into robust payload design and advancements in other spacecraft components?

This thesis describes the details of an idea that could be just that revolutionary. Countless satellites have failed early or reached what is today considered normal end-of-life due to degradation of their electrical power subsystems. Sometimes it's the batteries that fail, worn out from repetitive cycles of charging and discharging as the spacecraft goes in and out of eclipse. Other times the solar panels themselves, efficiency slowly but inevitably decreased by the harsh space radiation environment, are no longer able to generate enough electricity to operate power-hungry payloads.

Electrical power systems themselves are heavy and bulky, having to be overdesigned for beginning of life conditions. Satellite designers must plan for these degradations in battery and solar cell performance, sapping valuable weight and volume

that could be better spent on payloads. In addition, many satellites fail because they run out of propellant to perform orbit maintenance. Spacecraft engineers must make countless trade-offs between the size and mass of the payload versus the supporting components of the bus.

This thesis explains why power beaming from ground-based high-energy lasers to on-orbit spacecraft is such an attractive idea whose time has come. Various organizations, schools, and agencies have performed research in this area literally for decades. I have attempted to pull together the relevant results into a single, comprehensive document. Chapters describe solar cell design, the physics of laser power generation and propagation, electric propulsion concepts, and other related ideas. The thesis research effort culminated in a ground-based experiment with plans for an on-orbit extension.

A key to this thesis is that it is written, as much as possible, in plain easy-to-understand English. To a certain extent it has boiled difficult advanced concepts down to make them digestible to even a casual reader. It is intended to serve as a reference for future investigation, so that follow-on students and other researchers will have a portal into the vast body of knowledge that went into this one paper.

Revolutions rarely happen overnight. This thesis alone will not drastically alter the art and science of spacecraft design, but it will hopefully serve as a spark of inspiration to other engineers. The technology exists, the theory is sound—now it just up to us to take the risk to try something new and unproven. As Alan Kay wisely said, “The best way to predict the future is to invent it.”

II. GROUND-BASED LASERS

A. LASER CONCEPTS

The concept of the laser was first documented in 1957 (Kuhn, p. 4). In less than fifty years lasers have become ubiquitous in our world. Laser applications abound; scanning bar codes on food at the grocery store, playing recorded music or pictures on CDs and DVDs, handheld laser pointers used in presentations--people today accept lasers as part of their lives. Specialized lasers are also used in precision surveying, creating awesome effects in dance clubs and at outdoor laser light shows, illuminating targets for precision-guided bombs, creating holograms, and countless other applications. Higher-powered lasers are used in industry for cutting, welding, and etching, and are also being considered for many military missions.

The concept of the laser is so basic that it is now taught in many high school physics programs. As Kuhn explains, most lasers consist of a gain material, a pumping source, and output optics. (p. 19)

The gain material contains the atoms that will be excited and then participate in stimulated emission. Different lasers use solid matters, liquids, gases, or even plasmas as their gain materials.

A pumping source is used to inject the energy that elevates atoms to their excited states such that lasing can occur. Common pumps are optical, electrical, or chemical, but jet engines and conventional explosions have been used with nuclear explosions considered for X-ray lasers.

Finally, a resonant cavity is sometimes used to amplify the beam and set up the standing wave which is required for most moderate- to high-power lasers. Most resonant cavities include two mirrors that can be either planar or curved. Once the pumping source excites electrons and they then return to their normal energy state, they emit a photon at a specific wavelength but in a random direction. This spontaneous emission in all directions results in *some* photons being emitted in the direction of the mirrors. Those photons bounce back and can stimulate emission of other photons in the same direction and phase. These photons are reflected again and stimulate yet more coherent photons, setting up a standing wave.

Resonant cavities can be either stable or unstable. In a stable cavity, one of the mirrors is as completely reflective as possible while the other allows a tiny amount of transmission, say 1%. The 1% of the laser energy that makes it through the mirror is what is emitted, so a 5 mW laser may actually have 500 mW of energy within its cavity.

This approach is clearly impractical for high-energy lasers. When emitting beams in the megawatt-range, this would require hundreds of megawatts or even gigawatts of energy in the cavity which would destroy mirror coatings and essentially destroy the laser. High-energy lasers either do not use a reflective cavity or use an unstable cavity. In an unstable cavity, the light bounces several times within the cavity but eventually the entire beam escapes. One example of an unstable cavity is shown below in Figure 2.1, which is a reproduction of figure 4.23 from Kuhn:

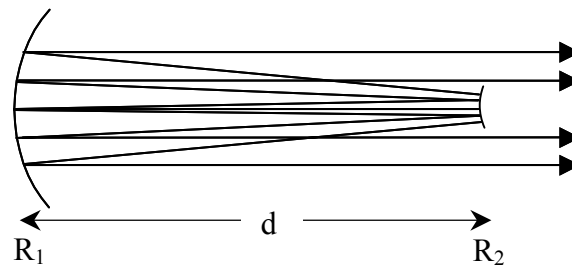


Figure 2.1 Unstable Resonator Schematic (Kuhn, p. 112)

This is a common type of unstable resonator with a large mirror on one end and a small mirror on the other. The energy that escapes around the smaller mirror becomes the output beam, which is donut-shaped.

The stability of a laser cavity is determined by the radii of curvature of the two mirrors (R_1 and R_2) and the distance between them (d). Stable cavities satisfy the equation (Kuhn, p.114)

$$0 < \left(1 - \frac{d}{R_1}\right) \left(1 - \frac{d}{R_2}\right) < 1.$$

A laser produces energy through the gain process. Each pass through the gain cavity increases the intensity of the coherent light. If we consider that electrons in the

atoms of the gain material can be in either their ground state (state 1) or excited state (state 2), there are three Einstein coefficients corresponding to rates of excitation and decay. (Einstein) These are the spontaneous emission rate (A_{21}), the stimulated emission rate (B_{21}), and the induced absorption rate (B_{12}). In equilibrium the rates of decay are equal to the rate of absorption, i.e., spontaneous emission plus stimulated emission equals induced absorption. (Kuhn, p. 53)

$$g_2 A_{21} e^{\left(\frac{-h\nu_2}{k_B T} \right)} + g_2 B_{21} e^{\left(\frac{-h\nu_2}{k_B T} \right)} \rho(\nu) = g_1 B_{12} e^{\left(\frac{-h\nu_2}{k_B T} \right)} \rho(\nu)$$

The fundamental law of thermodynamics states that when a collection of atoms is in thermal equilibrium at a positive temperature T , the relative populations of any two energy states E_1 and E_2 are

$$\frac{N_2}{N_1} = \frac{g_2}{g_1} e^{\left(\frac{E_2 - E_1}{kT} \right)}.$$

This means that the upper level population is *always* smaller than the lower level population, and we must therefore pump to a nonequilibrium condition. (Siegman, 1986)

Three- and four-level lasers use the exact same physics but with more than just one excited energy level. For example, the pump in a three-level laser may excite an electron to state E_3 from where it quickly decays to state E_2 . It can remain in this quasi-stable state until stimulated emission is induced, dropping it back to the ground state E_1 . (Walters)

Multi-state lasers are useful because, assuming quantum efficiency is not sacrificed to a large extent, the population inversion is maintained for a long time (in a quantum mechanical sense) and thermal transitions from the ground state to the lower laser state are minimized. (Biblarz)

When lasing action is in progress, it is no longer a steady-state condition. The gain coefficient $\gamma(\nu)$ is defined as the natural logarithm of the ratio of the intensity after a pass through the medium to the intensity before the pass divided by the distance of the pass. (Kuhn, p. 56)

$$\gamma(\nu) = \frac{1}{z} \ln \left(\frac{I_{end}}{I_{start}} \right)$$

It can also be defined in terms of energy states.

$$\gamma(\nu) = g(\nu) \left(\frac{A_{21} \lambda_0^2}{8\pi n^2} \right) \left(N_2 - N_1 \left(\frac{g_2}{g_1} \right) \right)$$

This form shows that to achieve gain, there is a need for a population inversion where there are more electrons in the excited state than in the ground state. All of the other terms (the Einstein coefficient A_{21} , the laser wavelength λ_0 , the index of refraction n , and the degeneracies g) are properties of the gain material itself.

The wavelength of light emitted from a laser (λ_0) depends on the gain material that is used. Since different materials contain electrons or molecules that can be excited to various energy levels that then decay to their ground states, the energy of the photon that is released will depend on the material. There are lasers that emit energy in almost all portions of the electromagnetic spectrum, although visible and infrared lasers are the most useful and therefore the most common. The table below (Lasers and Optonics Buying Guide) lists some of the most common laser materials used in high-energy lasers and their wavelengths.

Laser Material	Wavelength (μm)
Neodymium: YAG (Nd: YAG)	1.064
Iodine (I)	1.315
Hydrogen Fluoride (HF)	2.8
Deuterium Fluoride (DF)	3.8
Carbon Dioxide (CO ₂)	10.6

Table 2.1 Common High-Energy Lasers

Although iodine, HF/DF, and CO₂ lasers are all gas lasers, neodymium lasers are solid-state. Solid-state lasers usually achieve their high power through Q-switching or mode locking. These techniques can both be used to create abnormally large laser pulses at the expense of pulse repetition rate.

Q, or the quality factor of a laser cavity, measures the capability to store electromagnetic energy. Lasers with a high quality factor store energy well inside the cavity, while lower Q lasers emit energy rapidly from the cavity. “Q-switching is accomplished by placing something in the cavity that makes the cavity opaque (reduces the Q), so that laser action cannot occur. Since there is no laser action to reduce the population inversion, then the threshold inversion can increase to a level substantially higher than in the steady-state. If the cavity is suddenly returned to a normal transmissive condition, the increased population inversion will result in an increase in the gain and a dramatic increase in the photon density in the cavity.” (Kuhn, p.177)

The four technologies used in Q-switching are mechanical (a device which physically blocks the laser beam and can spin or swing out of the way), electro-optic (birefringent crystals that have different coefficients of refraction in orthogonal directions), acousto-optic (photoelastic materials which exhibit a change in the index of refraction when acoustically excited), and dye (absorbs at low intensities but bleaches to become more transparent at higher intensities). (Kuhn, pp.183-193)

Mode-locking technologies are similar to Q-switching ones, although the intermediate goal is somewhat different. In mode locking, all of the longitudinal modes are tuned to a constant phase difference. This is done by adjusting the cavity such that pulses separated by $2nL/c_0$ are produced. (Kuhn, p. 198)

B. GROUND-BASED HIGH-ENERGY LASER FACILITIES

The United States has the world’s most advanced facilities for laser research and applications. Academic, government, and military organizations own and operate these sites for a myriad of applications and users. While building lasers, even high-powered ones, has become a commodity operation, propagating those laser beams through precise optics and into space and tracking moving satellites is still a tricky business. There are only a handful of places in the world that can do it reliably and regularly.

1. MIT/LL Firepond Research Site

The Firepond Optical Facility is located at 42.6°N, 71.5°W near Westford, MA and is operated by the Massachusetts Institute of Technology's Lincoln Laboratories (MIT/LL). MIT/LL is a Federally-Funded Research and Development Center (FFRDC) that is chartered to perform research and other functions that cannot better be performed by contractors or government laboratories.



Figure 2.2 Firepond Lidar in Action

Laser propagation to space at Firepond started with the Clemson University/MIT Light Detection and Ranging (lidar) project funded by the National Science Foundation

(NSF). This lidar (shown in Figure 2.2) used a 25W, 31.7 Hz pulsed Nd:YAG laser to observe Rayleigh scattering in the atmosphere up to about 85 km. (Meriwether) The most modern instrument at Firepond is a lidar system designed, built, and operated by Thomas J. Duck and Dwight Sipler. This lidar was primarily used for day and night measurements of middle-atmospheric temperatures and gravity waves. “An important accomplishment was the first ever Rayleigh lidar observation of a mesospheric inversion layer in daytime.” (Duck)

Duck and Sipler’s work (shown in Figure 2.3) expanded on the experiments run by the Clemson/MIT team. Their higher power laser and cleaner optical path enabled more precise measurements and at higher altitudes than the earlier work.

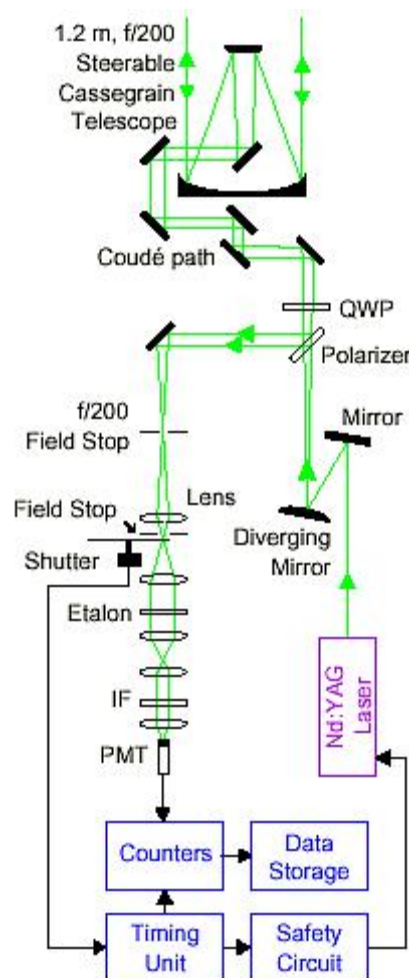


Figure 2.3 Firepond Lidar Schematic Diagram



Figure 2.4 Spectra-Physics GCR-6 Laser at Firepond

As shown in Figure 2.4, the laser is Nd:YAG, but it is a powerful injection-seeded frequency-doubled (532 nm) Spectra-Physics model with a 30 Hz pulserate that operates at 10 MW peak power.

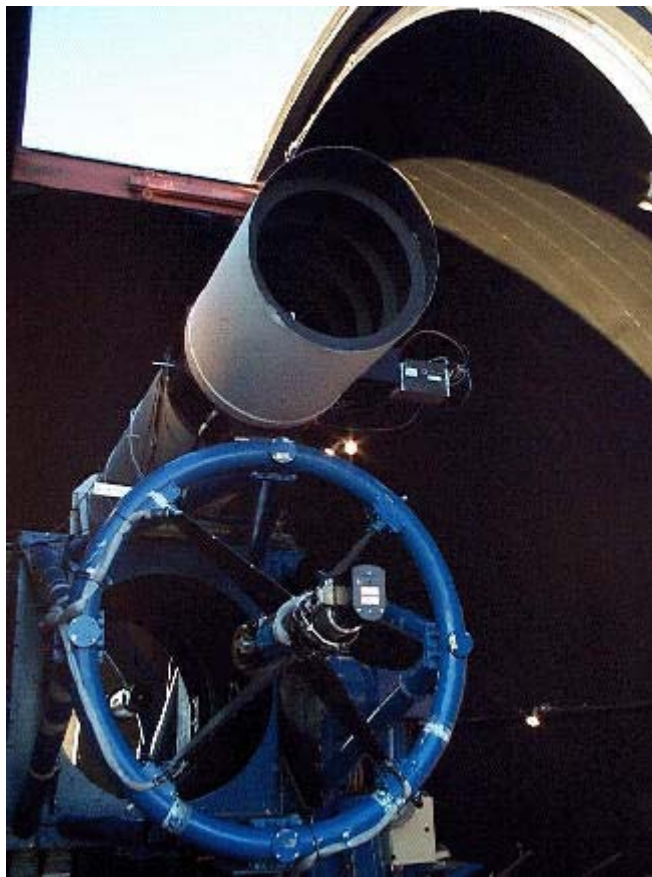


Figure 2.5 Firepond 1.2 meter Telescope

This laser is propagated using the Firepond 1.2 m aperture telescope (Figure 2.5), resulting in a narrow 0.1 mrad field of view.

2. Air Force Maui Optical and Supercomputing Site (AMOS)

The AMOS is a set of locations on the island of Maui operated by the Air Force Research Laboratory (AFRL). The Maui High-Performance Computing Center (MHPCC) is located in Research Park in the city of Kihei, while the optical station itself is located atop Mount Haleakala and is used for both research purposes and operational space situational awareness (SSA) for the Air Force Space Command (AFSPC).

There are many telescopes (shown in Figure 2.6) the site uses for optical tracking of space objects, most notably the 3.67 meter Advanced Electro-Optical System (AEOS) which became operational in 2000. There is also a 1.6 m telescope, two 1.2 m telescopes, two 1.0 m telescopes, a 0.8 m beam director/tracker, and a 0.6 m laser beam director. (Pike) Lasers can be fired at elevation angles as low as -5° depending on other conditions, meaning there is no theoretical limit on what satellite orbits can be reached from the site. (Skinner)



Figure 2.6 AMOS Telescopes

There are several lasers on site at AMOS that are used for lidar research, active tracking, and other purposes. There is a 9 J CO₂ laser, a 0.35 J tunable alexandrite laser, a 6 W tunable argon ion laser, and a 4.7 W tunable krypton laser on site. In addition, the High Performance CO₂ LIDAR for Space Surveillance (HI-CLASS) laser operates at 30 J and 30 Hz. (AMOS)

In the past, a 500W Holobeam Nd:YAG laser was used for high-energy experiments. That laser has since been moved back to the mainland, but in summer 2002 a new Ytterbium in yttrium argon garnet (Yb:YAG) laser will be installed that operates in different modes from 500 W to 1000 W depending on desired beam quality. This laser operates at 1.03 μm and can be frequency doubled to operate at 535 nm. (Snodgrass)

Mount Haleakala offers the distinct advantage of being at 3,058 meters elevation (over 10,000 feet), reducing the amount of atmosphere a beam must travel through to get to space. The climate is favorable and stable virtually year-round, and there is minimal scattered light from surface sources. In addition, the thermal soak of the Pacific Ocean for thousands of miles in every direction greatly reduces atmospheric turbulence, leading to extremely good seeing conditions (on the order of 1 arc second) for a terrestrial site. (AMOS)

AMOS is also well-suited to outside experimenters using the facility. In particular, AEOS was designed with modularity in mind. Multiple sets of research can take place simultaneously in rooms arranged under the telescope itself. Such visiting experiments pay a small fee for site support and overhead. Technical and administrative support is provided from offices at Premier Place, a technical park in Kihei, Maui.

Also atop Mount Haleakala are NASA's Lunar Ranging Experiment (LURE) facilities (shown in Figure 2.7), operated by the University of Hawaii. LURE has more recently been used for satellite ranging experiments using low power lasers. (O'Gara)



Figure 2.7 LURE Telescopes

3. White Sands Missile Range (WSMR) High-Energy Laser Systems Test Facility (HELSTF)

The U.S. Army Space and Missile Defense Command (SSDC) operates the WSMR HELSTF “to support test and evaluation of high-energy laser systems, subsystems, and components, and to support the conduct of damage and vulnerability tests on materials, components, subsystems, and systems.” (WSMR PA)

HELSTF (shown in Figure 2.8) was established in the 1970’s and first used as the test site for the Navy’s SEALITE program. TRW, under contract to the SEALITE program, built the Mid-Infrared Advanced Chemical Laser (MIRACL), a continuous wave (CW) DF laser operating at $3.8\ \mu\text{m}$. It is the highest power continuous output laser in the United States, operating in the megawatt-class (Talbot puts the total output power at 2.2 MW).

“The laser is basically an exotic rocket engine composed of individual module assemblies each having many nozzle blades. The modules are fed from an upstream combustion chamber and are designed to produce an optically uniform downstream flow field as a lasing medium. A gaseous oxidizer is reacted with a fuel mixture and ignited in the combustor to produce fluorine. Deuterium is injected into the flow to chemically combine with the fluorine atoms and produce the required population of excited DF molecules upon which lasing is based.” (WSMR PA)



Figure 2.8 HELSTF Facilities

HELSTF is host to other laser programs, most notably the joint U.S.-Israeli Tactical High-Energy Laser (THEL) program which developed an operational system for theater missile defense. In addition, MIRACL (shown in Figure 2.9) was used in the fall of 1997 for a controversial ASAT research test. The laser was fired at MSTI-3, a U.S. satellite that was past its useful lifetime, to improve computer models used for planning protective measures for U.S. satellites. (Pike)



Figure 2.9 Inside the MIRACL Facility

HELSTF is nearly ideally located for high-energy laser testing. It is located in the south-central part of the WSMR, far from civilized areas or common air traffic routes. There is sunshine 350 days per year, and the dry desert climate provides for excellent seeing conditions most of the time. (HELSTF)

4. AFRL Starfire Optical Range (SOR)

The SOR (shown in Figure 2.10) is located atop a small peak at Kirtland AFB in Albuquerque, NM. It is the nation's, and most likely the world's, premier location for ground-to-space laser beam propagation research and experimentation. Dr. Robert Fugate, the technical director of the site, is a world-renowned expert in adaptive optics and personally pioneered and oversaw the development of laser guidestar imaging.



Figure 2.10 SOR Telescopes and Mounts

“The primary mission of the SOR is to develop and demonstrate optical wavefront control technologies. The SOR houses a 3.5 m telescope (one of the largest telescopes in the world equipped with adaptive optics designed for satellite tracking), a 1.5 m telescope, and a 1.0 m beam director. In addition to its primary research charter, the SOR also supports field experiments by others within the research community.” (SOR)

Dr. Fugate’s work with laser guidestar adaptive optics has led to dramatic increases in the performance of ground-based astronomical telescopes. Normally in adaptive optics systems, bright natural stars serve as “beacons” for the adaptive optics system. By looking at these beacons, the system can measure and correct for atmospheric distortions. Unfortunately, there are a limited number of suitable stars which do not completely cover the sky. Dr. Fugate has used a laser to measure the scattering from atmospheric molecules or a layer of sodium atoms 60 miles above the earth’s surface to

create an artificial beacon or guidestar in the direction of interest. (Fugate) One of these experiments is shown in action in Figure 2.11.



Figure 2.11 Laser Beacon Propagation from the 1.5 m Telescope

SOR, while not at as high an elevation as AMOS, is still located at an altitude of over 8,000 feet. The thermal environment, however, is much messier due to the mountainous nearby terrain, and the light produced by the nearby city greatly increases optical noise.

The government and contractor personnel working at the site are extremely knowledgeable, competent, and dedicated. They are used to working very long hours, have the ability to rapidly reconfigure test equipment when needed, and have more experience with satellite tracking and laser beam propagation to space than anyone else in the world.

In addition, there are a variety of lasers on site at SOR. Due to the dynamic nature of their mission and experiments, laser sources are constantly being added or removed. The following spreadsheet shows a snapshot in time of lasers installed and available at the site in July, 2002. (Johnson)

Laser	Output Power (W)	Wavelength (nm)	Divergence (1/e, half-angle) (μrad)	Pulse Width (nsec)	PRF (Hz)	Pulse Energy (J)
Antares	17	1064	0.3	CW	CW	CW
Argon	4	514.5	8	CW	CW	CW
ATLAS (IR)	400	1064	15 - 50	80000	2500	0.024
ATLAS (Doubled)	150	532	15 - 50	80000	2500	0.024
Coherent Verdi (5W)	5	532	5	CW	CW	CW
Coherent Verdi (10W)	6	532	6	CW	CW	CW
Lee	pulsed	532	14	150	2000	0.01

Table 2.2 Lasers Available at SOR

5. SELENE (Space Laser Energy)

The most visionary work done in this area appears to be that of the SELENE Corporation, a private company operating out of Lompoc, CA. Dr. Hal Bennett is the president of the company and is applying his Naval career expertise to making space power beaming a reality.

Unlike the other HEL sites previously mentioned, SELENE proposes to build a free-electron laser (FEL). Although the output of a FEL exhibits the same characteristics of laser light as any other laser, the amplification medium is not electrons bound to the gain medium but rather “free” electrons that have been stripped from atoms in an electron gun which are then accelerated to relativistic velocities.

“While the electrons are propagating through a long, periodic magnetic dipole array - a so called undulator - the interaction with an electromagnetic radiation field leads to an exponential growth of the radiation emitted by the electrons. This amplification of radiation is initiated by an increasingly pronounced longitudinal density modulation of the electron bunch. The initial radiation field can be an external one, e.g. a seed laser, or an ‘internal’ field, i.e., the spontaneous emission of the undulator. In the latter case it is called a SASE (Self Amplified Spontaneous Emission) FEL. Since the electrons in the FEL are not bound to atoms and thus not limited to specific transitions, the wavelength of

the FEL is tunable over a wide range depending on accelerator energy and undulator parameters.” (Feldhaus)

Figure 2.12 illustrates the FEL principle graphically.

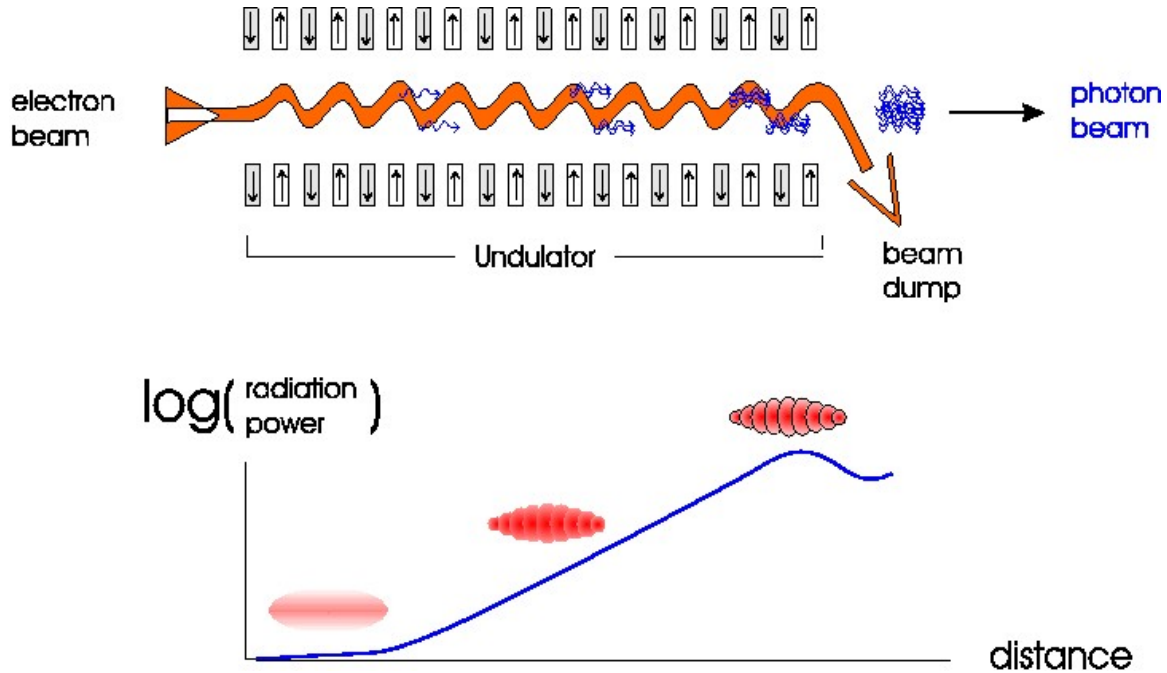


Figure 2.12 The FEL Principle

SELENE has proposed a ground-based infrastructure beaming power to a reusable “space tug” that will repeatedly transfer satellites from LEO to GEO and, if needed, back again. The SELENE concept includes a \$25M power beaming complex with a 12 m telescope and a Berkeley Lab-constructed, Russian-designed 200 kW free-electron laser in Ridgecrest, CA. The entire program, including the space tug, is estimated to cost \$350M. Currently the company has spent about ten million dollars on studies but has not yet broken ground. (Preuss)

C. CONCLUSION

For the experiments performed in this thesis, the Maui AMOS site was chosen. Although laser beaming to PANSAT was not accomplished due to extensive delays in the delivery of the Active Track Laser (a kilowatt-class one micron source that was to be

used to lase PANSAT), contacts at the site provided a lower-power source that could be used for ground-based experiments. Since the eventual goal of lasing PANSAT still exists, it made sense to begin the experiments on the same optics bench that will be used in follow-on work. In addition, it enabled on-site personnel to get familiar with the test series and Prof Michael, who will presumably oversee future work.

When considering ways to beam power to satellites or to perform laser annealing of radiation-damaged solar cells, ground-based sites offer many advantages. Weight and space considerations are not very important, maintenance of the laser and associated hardware is relatively simple, and the physical infrastructure is already in place in several locations.

Still, there are disadvantages associated with ground-based sites as well. Even the best ground sites have to propagate the laser beam through much of the atmosphere, forcing the use of adaptive optics and still resulting in tremendous losses. Predictive avoidance is complicated, and there are safety issues concerning people on the ground and aircraft in the vicinity. Raising the laser higher off the ground ameliorates some of these issues, but it also introduces additional challenges to overcome.

III. AIR- AND SPACE-BASED LASERS

A. LIMITATIONS OF GROUND-BASED LASERS

The best way to minimize the effects of diffraction and atmospheric turbulence is not to use adaptive optics but to actually have the laser beam path traverse less (or none) of the atmosphere. After all, if there is no beam distortion to correct then the maximum amount of power will reach the intended target.

Simple diffraction of the beam will result in much less power being delivered to a satellite at either LEO or GEO. In theory, the smallest possible divergence angle is the diffraction-limited case.

$$\theta_d = \frac{\beta\lambda}{D}$$

β is a coefficient that depends on the desired units for the answer (1.02 for radians and 58.5 for degrees), λ is the laser wavelength, and D is the beam diameter. (Kingsley) As an example, propagating a frequency-doubled Nd:YAG beam through the 3.5 meter telescope at the Starfire Optical Range would result in a diffraction-limited divergence angle of approximately 8.892×10^{-6} degrees, or about 0.032 arcseconds.

When dealing with angles this small, it is appropriate to estimate the beam diameter D at a target a distance L away from the emitter as $D = L\theta$. Continuing the example, this beam at PANSAT's altitude of roughly 530 km would have a diameter of about 8 cm. Assuming the laser puts out 150 W (and there are no losses between the ground site and the satellite), this would produce an irradiance of almost 7.5 MW/m²!

Of course as we strip away those simplifying assumptions and add more and more of the constraints of the real world, the irradiance drops dramatically. The Strehl ratio (I_{REL}) is a measure of how closely a laser beam performs to the diffraction limited case. It is a product of laser beam quality, track jitter, and turbulence compensation for higher-order phase distortions. (Fugate, p. 16) The goal of adaptive optics is to improve the Strehl ratio.

A more complete and accurate equation for the irradiance at the target is

$$H = I_{REL} \frac{P}{R^2} \frac{\pi}{4} \left(\frac{D}{\lambda} \right)^2$$

where P is the transmitted power, R is the range to the target, D is the beam diameter, and λ is the laser wavelength. Atmospheric turbulence alone reduces I_{REL} from 0.001 to 0.01. Without adaptive optics, power beaming is not a viable concept.

Figure 3.1, which depicts the performance of the largest telescope at SOR, assumes an r_0 , or atmospheric coherence length, of 5 cm. The r_0 is a measure of the seeing conditions at a site, which is dependent on many factors. Higher altitude sites and those in benign thermal conditions (such as AMOS) have better r_0 values than those in harsher environments (like SOR). This term describes the aperture of a diffraction-limited telescope that would have the same performance as the larger telescope under the less-than-ideal conditions. As this example indicates, the poor seeing conditions effectively reduce the 3.5 m telescope at SOR to a 5 cm diffraction-limited telescope. Under excellent conditions, SOR achieves r_0 values of 10 cm; AMOS routinely has r_0 values of 15-25 cm.

Dr. Bob Fugate, the technical director at SOR, ran several simulations to measure predicted irradiance at a LEO target satellite. These runs varied the Strehl ratio, elevation angle (and therefore range to target), laser power level, and laser wavelength. For example, a 532 nm, 130 W beam shot straight up would have a target irradiance of approximately 50 W/m². A 360 W, 1.064 μ m beam shot straight up would only provide about 25 W/m² at the target. This graphically demonstrates the impact of wavelength on divergence, as the higher power laser (which also passes through a more transparent part of the atmosphere) produces less irradiance at the target.

3.5-m Telescope Adaptive Optics Performance

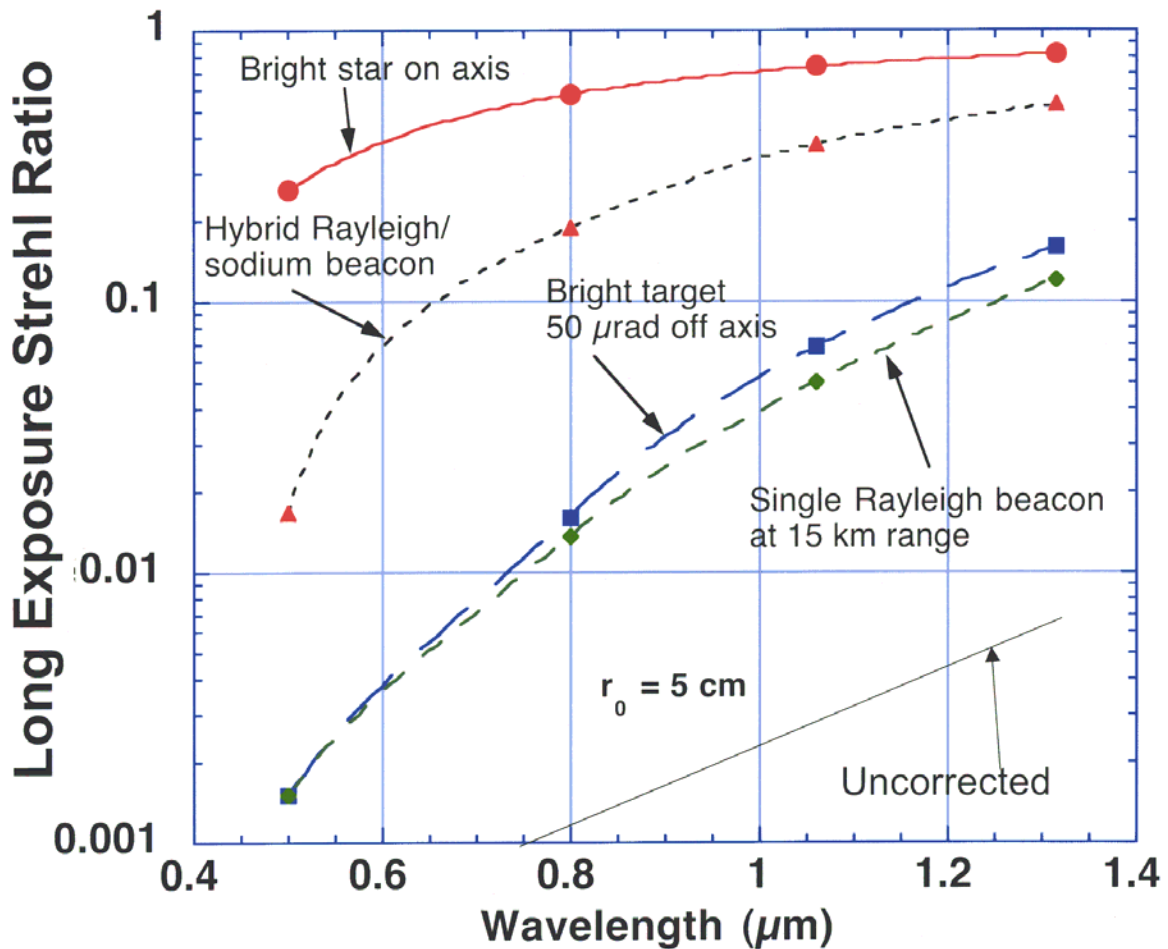


Figure 3.1 Strehl Ratio vs Wavelength

Laser wavelengths must be carefully chosen, as the atmosphere is transparent only in certain windows of the electromagnetic spectrum. Neodymium (1.06 μm) and iodine (1.315 μm) lasers fall in areas where the atmosphere is virtually transparent, as seen in Figure 3.2. (Clark)

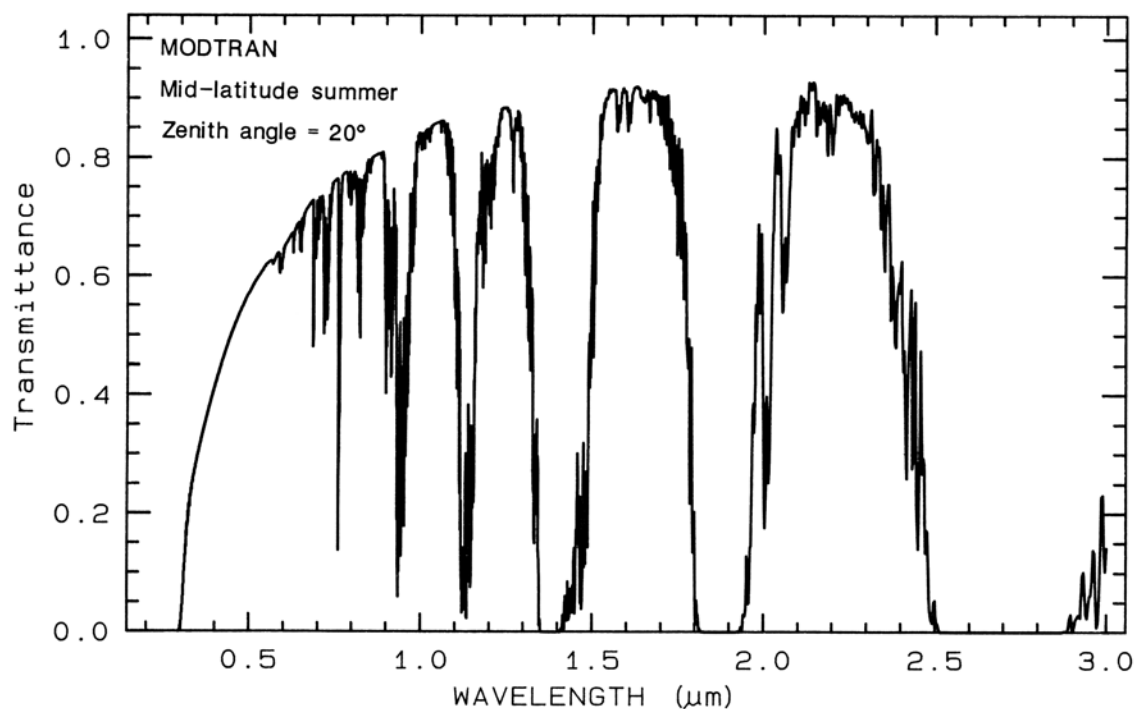


Figure 3.2 Atmospheric Transmission at Sea Level

The HF laser at 2.8 μm does not operate in a transmission window. In fact, the atmosphere is practically opaque at this wavelength. Water, carbon dioxide, and other elements and compounds in the atmosphere act as filters to certain colors of light. The DF laser, however, at 3.8 μm , has about 95% transmission. The CO_2 laser, operating at 10.6 μm , also sees about 95% transmittance through the atmosphere. A frequency-doubled Nd:YAG operating at 532 nm will transmit about 50% of its power through the atmosphere.

B. THE AIRBORNE LASER

Of course getting out of the atmosphere will eliminate these turbulence effects. The next best thing would be to get as high in the atmosphere as possible to greatly reduce these losses. Although the Air Force's YAL-1A Airborne Laser (ABL) is designed as a missile defense platform, it is conceivable (as shown in Figure 3.3) that the weapon-class laser on board could be directed upward and used for power beaming or solar cell annealing of spacecraft.



Figure 3.3 ABL Engaging a Target

The \$1.3B Program Definition and Risk Reduction (PDRR) contract for the ABL was signed on 12 Nov 96, with Boeing as the integrating contractor, Lockheed Martin responsible for the target acquisition and beam/fire control systems, and TRW responsible for the high-energy laser. The Air Force's ABL Program Office, part of the Aeronautical Systems Center, is managing the program out of Kirtland AFB, NM for the Missile Defense Agency (MDA), previously known as the Ballistic Missile Defense Organization (BMDO) and before that the Strategic Defense Initiative Organization (SDIO). (ABL)

The total acquisition program cost is currently estimated at \$11B for seven aircraft. (ACC/DR) As McCann's paper describes, the ABL actually has *four* lasers on board that operate in sequence in a successful missile kill.

Once the on-board infrared search and track (IRST) sensors detect a target, the active ranger system takes over. It consists of a 200 W continuous wave CO₂ laser that operates at 11.149 μm , a wavelength that was chosen to maximize atmospheric transmission. As the name indicates, this laser is used to measure the distance to a target. The track illuminator laser is a 10 W pulsed Yb:YAG laser operating at 1.0296 μm . It will initially be sized to a 5 m diameter at the target that will gradually be collapsed to a much smaller spot size. The beam control/fire control computers will "walk" this beam up the missile body to the nose. Next, the beacon illuminator laser, a kilowatt-class

pulsed Nd:YAG, will be propagated through the 1.5 m aperture nose turret to the target, measuring the atmospheric effects on the beam's wavefront. This is the signal which will allow adaptive optics to correct atmospheric turbulence when sending out the kill laser energy. The high-energy laser consists of multiple chemical oxygen iodine laser (COIL) modules, arranged in series to produce a megawatt-class 1.315 μm beam. Figure 3.4 shows a schematic of how the various systems are arranged in the aircraft.

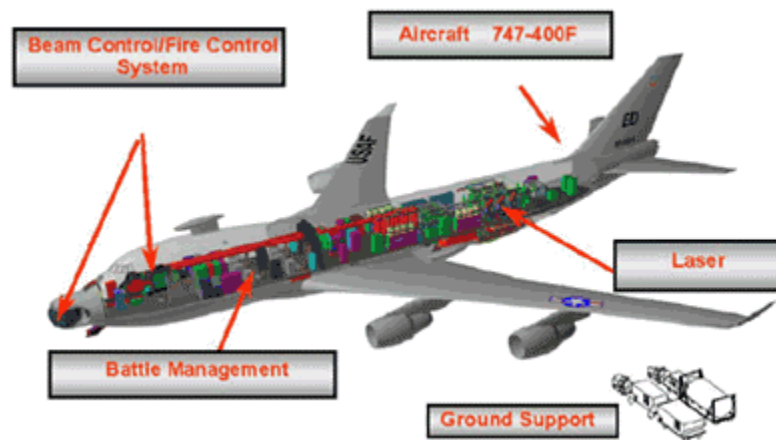


Figure 3.4 ABL Schematic Diagram

The ABL CONOPS calls for a mission altitude of 40,000 feet (approximately 12 km). Although this doesn't make a noticeable difference as far as beam divergence is concerned, it makes a big difference when it comes to atmospheric scattering and absorption.

Of course there are drawbacks to using the ABL for spacecraft power beaming. First and foremost, it is not the platform's primary mission. These aircraft are designed to orbit near a battlefield or threat area where there is risk of enemy missile launches. Using them to beam power to spacecraft would take away from their ability to perform this primary mission.

In addition, the beam control software must be modified to allow for tracking of satellites, although this should be a relatively simple enhancement to the software that is currently designed to track missiles. There is already a full satellite catalog on board for predictive avoidance purposes.

There are also political considerations. Any time high levels of directed energy are aimed at the heavens there are critics who claim the United States is militarizing space. Although these criticisms should not stop rational scientific progress, they must be taken into account.

Finally, a moving aircraft is certainly not the ideal platform for beaming power to space. Satellite tracking is complicated both by the 0.8 Mach motion of the aircraft and turbulence the aircraft itself flies through. Finally, despite adaptive optics, the laser beam must still pass through some atmosphere, leading to diffusion and thermal blooming losses.

C. THE SPACE-BASED LASER

Although the program has recently been drastically scaled back, the Air Force is also pursuing a space-based laser (SBL) for missile defense applications. For beaming power to other satellites, it completely solves the atmospheric turbulence and thermal blooming problems.

TRW is the lead contractor for the SBL program, which is funded by the MDA and run by a program office at the Air Force's Space and Missile Systems Center (SMC), part of the Air Force Space Command (AFSPC). It is the culmination of thirty years' research into high-energy lasers, beam control systems, precision optics, and fire control systems.

SBL will be a 4 m aperture megawatt-class HF laser operating at 2.8 μm . The atmosphere is opaque to this wavelength, meaning that beam scatter will be absorbed and will not reach the ground. This is one specific reason why an HF laser was chosen for the SBL rather than a COIL.

Although SBL (like ABL) is designed as a missile defense program, current architecture studies are considering the possibility of additional missions. Offensive counter space is specifically mentioned (SBL FAQ), meaning the SBL could have the inherent capability to direct high-energy laser light at other satellites. Power beaming would be a natural complementary mission.

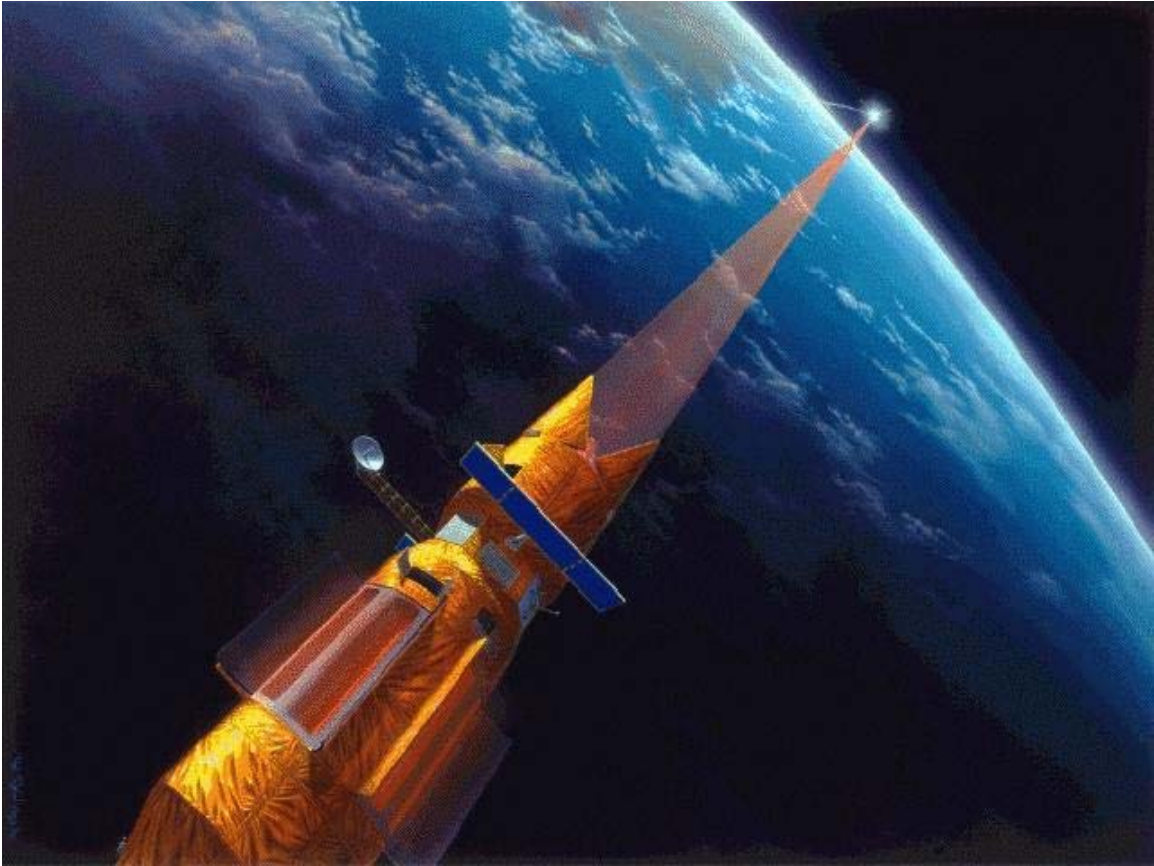


Figure 3.5 SBL Engages a Target

The SBL program (shown in Figure 3.5) is currently building a \$3B integrated flight experiment (IFX), scheduled for launch in 2012 with a lethality demonstration planned the next year. (IFX Fact Sheet, 2002) The operational SBL constellation is envisioned to have 20 satellites operating at a 40° inclination, providing full-time worldwide coverage. (SBL)

Assuming the diffraction-limited case, SBL would be able to impart tremendous amounts of energy to other satellites. In fact, given notional numbers for orbit altitude and assuming a 1 MW output, it could beam 40 MW/m^2 to satellites in GEO orbit! Unfortunately, any current solar cell technology demonstrates 0% conversion efficiency at the long wavelength of an HF laser. To be feasible, new satellites would have to include completely dedicated power conversion equipment to use this laser light.

IV. ELECTRIC PROPULSION

A. INTRODUCTION

Ever since the advent of the space age, chemical propulsion has pushed satellites into orbit, kept them there, and helped get them out of useful orbits when their lifetimes were complete. Both solid and liquid rocket boosters are now familiar sights, standing tall and proud on launch platforms. Bipropellant thrusters provide the ΔV needed to change orbital parameters such as altitude or inclination, while monopropellants like hydrazine are suitable for attitude control.

Researchers have been looking for many years at employing electric propulsion systems for attitude control, and more recently for orbit maintenance and changing. The former Soviet Union used Hall-effect electric propulsion in many of their satellites, and the United States is now adapting Russian technology for use on our spacecraft.

The NASA Office of Space Science provides a good overview of electric propulsion technologies. There are three basic types of electric propulsion systems: electrothermal, electrostatic, and electromagnetic. In electrothermal propulsion, an electric arc or resistance heater warms the propellant. The hot propellant is then exhausted through a conventional rocket nozzle to produce thrust. In electrostatic propulsion, a gaseous propellant is ionized and accelerated to high exhaust velocity in an electric field. A series of high-voltage electrically charged grids creates the electric field. In electromagnetic propulsion, the $\mathbf{j} \times \mathbf{B}$ forces accelerate an ionized plasma.

Electrostatic ion propulsion is the most developed. The electrical power required can be generated by either solar arrays or a nuclear reactor. Electric propulsion systems have high specific impulse, but very low thrust. This means that spacecraft can achieve high final velocities from a small amount of propellant if the electric propulsion system thrusts continuously over a long period of time.

Performance of ion propulsion systems can be improved by using high molecular weight propellants such as Xenon and C^{60} . Carbon-carbon accelerator grids that reduce erosion can increase lifetime. (Mucklow)

Of course there are advantages and disadvantages to electric propulsion. The biggest advantage is the very high specific impulse (compared to chemical rockets)

produced, meaning they can operate for a long time without using much fuel. One major disadvantage is that the thrust produced is extremely small—on the order of millinewtons. Table 4.1, adapted from Figures 17-4 and 17-5 of SMAD (pp. 692-693), summarize these qualities.

Type	Propellant	Vacuum I_{sp} (sec)	Thrust (N)	Average Density (g/cm^3)	Advantages	Disadvantages
Solid Chemical Motor	various	280 - 300	50 – 5×10^6	1.80	simple, reliable, relatively low cost	limited performance, higher thrust, safety issues, performance not adjustable
Monopropellant Chemical	H_2O_2 N_2H_4	150 - 225	0.05 - 0.5	1.44 1.0	simple, reliable, low cost	low performance, higher weight than bipropellant
Bipropellant Chemical	O_2 and H_2	450	5.0 – 5×10^6	1.14, 0.80	very high performance	cryogenic, complicated
Arcjet Electrothermal	NH_3 , N_2H_4 , H_2	450 – 1500	0.05 – 5.0	0.6, 1.0, 0.019	high performance, simple feed system	high power, complicated interfaces
Ion Electrostatic	Hg/A/ Xe/Cs	2000 – 6000	5×10^{-6} – 0.5	13.5/0.44 2.73/1.87	very high performance	very high power, low thrust, complicated
Hall Effect Electrostatic	Xe	1500 – 2500	5×10^{-6} – 0.1	0.22	high performance, high power/thrust density	high development risk, high power, complicated

Table 4.1 Propulsion Systems Comparison

Electric propulsion systems operate under the same basic theory as chemical rockets—a mass is accelerated in a certain direction such that conservation of momentum pushes the spacecraft in the opposite direction. The difference is that the ions or the plasmas that are accelerated are quite light compared to the mass of chemical combustion products (or of the spacecraft). Their extremely high velocities make up for part of this difference.

The efficiency of an electric propulsion device is defined as the ratio of kinetic energy expelled to the input energy (Wertz, p. 702).

$$\eta = \frac{\dot{m} v^2}{2P}$$

In this equation, η represents the overall efficiency, \dot{m} is the mass flow rate, v is the exhaust velocity, and P is the input power. Differing electric propulsion concepts will

require various amounts of input power and propellant mass, although in all cases the mass will be far lower than for any chemical thruster. In general, Hall-effect thrusters appear to be optimal for typical Earth-space missions. (Wertz, p.708) A key concept to keep in mind is that the thrust output of an ion thruster is directly proportional to the power input. If there were a way (such as through laser illumination) to increase the current or voltage sent to the electric thruster from solar panels, it would produce a correspondingly larger thrust.

B. APPLICATIONS OF ELECTRIC PROPULSION

As stated earlier, the two main applications of electric propulsion systems are in stationkeeping/orbit maintenance and in orbit changing (boosting to and from mission orbits).

1. Electric Propulsion for Stationkeeping

In 1997, Boeing started marketing a xenon ion propulsion system (XIPS) with two of their standard buses. XIPS (Figure 4.1) replaces the standard chemical propulsion used for stationkeeping. “The increased efficiency possible with XIPS allows for a reduction in propellant mass of up to 90% for a satellite designed for 12 to 15 years operation. Less propellant results in reduced cost for launch, an increase in payload, or an increase in satellite lifetime, or any combination of the above.

Small thrusts are required to correct for the tug of solar or lunar gravity and to reposition the satellite in its proper orbit and altitude. A satellite's lifetime as well as its launch weight is thus determined by the amount of fuel aboard for its thruster system.

While most current satellites use a chemical bipropellant propulsion system, a XIPS-equipped satellite instead uses the impulse generated by a thruster ejecting electrically charged particles at high velocities. XIPS requires only one propellant, xenon, and does its stationkeeping job using a fraction of that required by a chemical propellant system.

The heart of the XIPS is the ion thruster, measuring less than 10 inches across. Two other key units include a tank containing xenon gas and a power processor.

Thrust is created by accelerating the positive ions through a series of gridded electrodes at one end of the thrust chamber. The electrodes, known as an ion extraction assembly, create more than 3,000 tiny beams of thrust. The beams are prevented from being electrically attracted back to the thruster by an external electron-emitting device called a neutralizer.

Ions ejected by the Hughes-designed XIPS travel in an invisible stream at a speed of 30 kilometers per second (62,900 miles per hour), nearly 10 times that of its chemical counterpart. And, because ion thrusters operate at lower force levels, attitude disturbances during thruster operation are reduced, further simplifying the stationkeeping task.

Chemical thrusters in use today are limited by how much energy is released during the combustion process. Ion thrusters are dependent on the amount of electrical power available. More power means faster-moving ions and higher thrust. The Boeing 601HP XIPS uses 500 watts from the satellite's 8-kilowatt solar array. For the Boeing 702 model, XIPS uses 4,500 watts from the 10- to 15-kilowatt solar array. XIPS operations have no effect on broadcasting and telemetry operations.

A typical satellite will use up to four XIPS thrusters (two primary, two redundant) for stationkeeping, all connected to the same xenon supply. Each primary device will be switched on and off by a smart power unit that monitors and diagnoses operations automatically. In normal operation, each Boeing 601HP ion thruster will operate for approximately 5 hours per day. Each Boeing 702 ion thruster will operate for approximately 30 minutes per day.

The Boeing 601HP satellite uses the 13-centimeter XIPS to perform all north-south stationkeeping and spacecraft momentum control in two axes. The 13-centimeter thruster operates at a specific impulse rate (ISP) of 2568 seconds with 18 millinewtons (mN) of thrust. The satellite flies four 13-centimeter xenon thrusters and two power processor units. Orbit and momentum control are accomplished through a series of two burns on each day of the stationkeeping cycle. Only two of the four thrusters are required to perform a complete mission of on-orbit maneuvers.

The Boeing 702 uses its high-power capacity to take full advantage of XIPS technology with the previously developed higher-power 25-centimeter thrusters. The 25-

centimeter thruster operates at an ISP of 3800 seconds with 165 mN of thrust. The satellite flies four 25-centimeter thrusters and two XIPS power processors. The HS 702 uses the XIPS to perform all stationkeeping and spacecraft momentum control. Like the HS 601HP, only two of the four thrusters are required to perform the entire on-orbit mission maneuvers. These functions are accomplished autonomously with a series of four daily burns providing precise orbit control. This strategy maintains a ± 0.005 degree stationkeeping box, allowing for collocation of many satellites in a single orbital slot.” (Boeing PR)

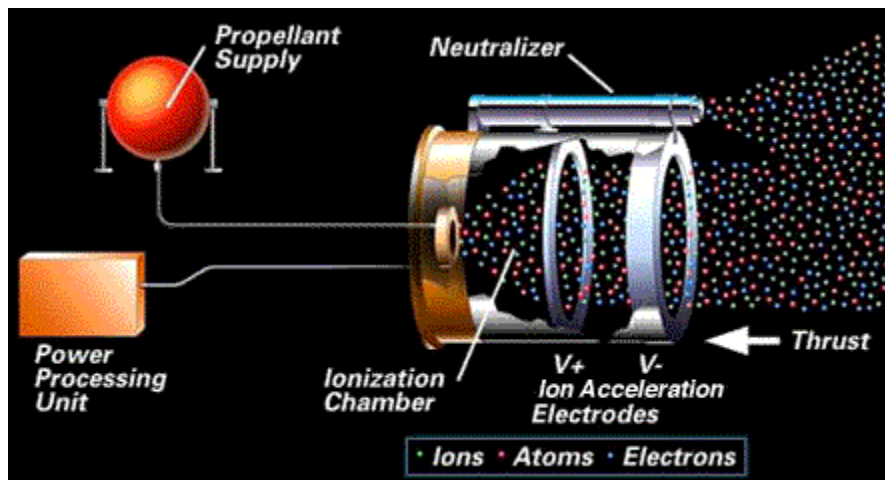


Figure 4.1 Boeing XIPS Schematic Diagram

There are other vendors with similar products on the market. In fact, the December 2001 issue of the AIAA Journal Aerospace America states that “every major commercial U.S. and European builder of geosynchronous satellites now offers electric propulsion as an option for stationkeeping, and some offer it to accomplish part of orbit raising.”

2. Electric Propulsion for Orbit Raising

In some cases, the stationkeeping thruster could also be used for orbit raising. The drawback is that the low thrust makes for long orbital transfer times, but in some cases this is acceptable.

“The Boeing 702 offers the additional option of XIPS orbit raising. Using XIPS to augment transfer orbit further reduces the amount of chemical propellant loaded. Larger payloads can thus be accommodated, with greater flexibility in the choice and use of a launch vehicle. Chemical propellant is used to place the satellite into a supersynchronous elliptical transfer orbit, and pre-programmed XIPS maneuvers are used to circularize the orbit and position the satellite in its final orbit.” (Spitzer)

The main benefit here is to reduce the propulsion system mass such that more mass fraction can be allocated to the payload. Or, the reduced mass may enable launch from a smaller, less expensive booster. In some cases, so much mass can be saved that multiple satellites can be launched on the same launch vehicle, dramatically reducing a system’s overall cost.

One concept for a feasible near-term solution involves using a traditional expendable launch vehicle to get to the geosynchronous transfer orbit (GTO), then firing the on-board chemical apogee system to place the satellite in an inclined orbit with apogee above GEO altitude and perigee above the Van Allen belts, then using Hall effect thrusters to raise the perigee, lower the apogee, and change the plane. Several satellite providers plan to use this orbit insertion technique, which will take one to two months and enable a payload weight increase of 20% to 35%. (Oleson, p. 6)

Oleson also describes a concept that eliminates the need for an expendable upper stage. This 60-day insertion enables stepping down from an Atlas launch vehicle to a Delta, cutting launch costs approximately in half. In the far term, he envisions 50 kW thrusters that take the satellite directly from LEO to GEO in a few months’ time, enabling the payload mass to increase by almost four times. (Oleson, pp.7-8)

Finally, Ziemer describes an ablation microthruster concept where a less than ten watt laser ablates (wears away) material such as Teflon which is ejected to generate a small amount of thrust. These systems have successfully lifted microsatellite-weight objects hundreds of feet into the air.

As far back as 1965, NASA has been interested in laser power transmission, “quite simply because it may ultimately allow space missions which would be impossible by other means.” Nored goes on to say, “Of particular interest to NASA is the

transmission of power over long distances for applications such as direct conversion to propulsive thrust or electrical power.”

More recently, the Air Force Research Lab (AFRL) determined that one could use 370 kW continuous wave lasers to deliver 110 kW of energy for orbit transfer applications. Four sites worldwide with 4 meter beam directors would enable the transit to be completed in about forty days. This is in comparison to a typical chemical thruster transfer which takes one to three days.

3. Electric Propulsion for Orbital Maneuvering

Electric propulsion can also enable novel ideas for changing the orbits of satellites once they have been launched. Today, it takes so much chemical fuel to change the subsatellite point of a GEO satellite that such maneuvers are only performed in the gravest of situations (e.g. shifting a Defense Support Program (DSP) satellite to provide better coverage in support of the Gulf War). Such maneuvers are costly because they greatly reduce the lifetime of the affected satellite. Fuel that is normally saved for years of stationkeeping is burned quickly, and these maneuvers can never be performed more than once.

With ion thrusters, however, this is no longer a critical concern. Satellites could be retasked at will, and not just in the GEO belt. Satellites launched into high orbits could be brought back down for on-orbit servicing or even collection into the Space Shuttle cargo bay to be returned to Earth. There are myriad space control applications for easily maneuverable satellites, not the least of which is making their exact orbit unknown to make targeting by hostile forces much more difficult. Repositioning existing assets is both faster and more economical than launching new satellites, and lasers powering an electric propulsion system can cut maneuver times in half. (Lipinski)

Laser power can also enhance solar flux for other applications. The average commercial GEO communications satellite costs \$250M and earns \$25M to \$50M per year. They are in eclipse for ninety days a year for up to seventy minutes at a time. Rechargeable batteries are used to power the spacecraft during eclipse, but they are the most common failure item. In addition, these batteries are heavy. Twenty percent of the mass of a typical GEO communications satellite is the power system and over half the

mass of the power system has no other function than to provide power during eclipse. Eliminating the need for energy storage (which is needed less than one percent of the time) would reduce the satellite mass by ten percent, enabling a smaller launch vehicle or more mass for the payload. Bamberger studied this approach, concluding that missile tracking sensors, space-based lasers, and space-based radars would all see significant payload mass benefit from using a power beaming approach.

Although lasers can be used during eclipse to replace the power flux produced by the sun, they can also supplement the sun's energy when the satellite is not in eclipse. This can further reduce the time required for orbit transfers or enable high power demand applications. Of course satellites would have to be designed to take advantage of such higher power output, and they could also include photovoltaic arrays that are highly efficient at light wavelengths that can be easily produced on the ground.

In fact, one of the competing technologies to laser power beaming is microwave power beaming. The concept is exactly the same, except that satellites already have photovoltaic power conversion systems. Implementing a microwave power beaming apparatus would require a whole new satellite subsystem and R&D in as-yet unexplored areas. In addition, Michael says that microwave power conversion systems are far less efficient than light to power converters. Laser power beaming is clearly the way to go.

V. PHOTOVOLTAIC CELLS

A. SOLAR CELL TECHNOLOGY

The vast majority of artificial earth-orbiting spacecraft use photovoltaic solar cell technology as their primary means of electrical power generation. In fact, the second satellite the United States ever launched, VANGUARD I which was sent up on 17 Mar 58, used photovoltaic cells to provide 100 mW of power for eight years of operation. (Loke) These pioneering cells had a conversion efficiency of 10%. (Rauschenbach, p. 1.1-1) Ever since, as power requirements have risen, so have the size and efficiency of solar cell arrays.

Solar cells (illustrated in Figure 5.1) rely on the photovoltaic effect, a basic physical process by which the cells convert sunlight to energy. As Seale explains, "Sunlight is composed of photons, or "packets" of energy. These photons contain various amounts of energy corresponding to the different wavelengths of light. When photons strike a solar cell, they may be reflected or absorbed, or they may pass right through. When a photon is absorbed, the energy of the photon is transferred to an electron in an atom of the cell (which is actually a semiconductor). With its newfound energy, the electron is able to escape from its normal position associated with that atom to become part of the current in an electrical circuit. By leaving this position, the electron causes a hole to form. Special electrical properties of the solar cell, a built-in electric field (thanks to a P-N junction), provide the voltage needed to drive the current through an external load (such as a light bulb)."

Of course the external load can also be the power-drawing equipment on a spacecraft. For space applications, solar cells are very slightly different from those employed in terrestrial use. The difference primarily involves the addition of a very thin layer (on the order of 10-30 mils) of cover glass which provides a measure of radiation shielding to protect the cell from the harsh effects of the radiation environment in space.

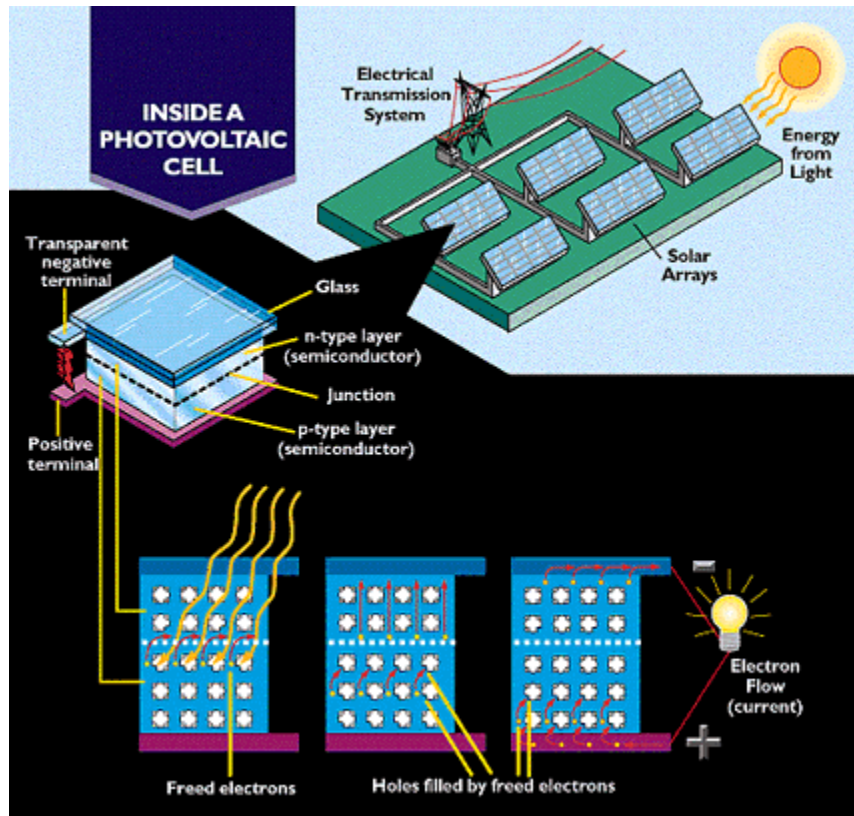


Figure 5.1 Inside a Photovoltaic Cell (image courtesy DoE)

Seale goes on to say, “Modern solar cells are based on semiconductor physics -- they are basically just P-N junction photodiodes with a very large light-sensitive area. The photovoltaic effect, which causes the cell to convert light directly into electrical energy, occurs in the three energy-conversion layers. The first of these three layers necessary for energy conversion in a solar cell is the top junction layer (made of N-type semiconductor). The next layer in the structure is the core of the device; this is the absorber layer (the P-N junction). The last of the energy-conversion layers is the back junction layer (made of P-type semiconductor).

As may be seen in the above diagram, there are two additional layers that must be present in a solar cell. These are the electrical contact layers. There must obviously be two such layers to allow electric current to flow out of and into the cell. The electrical contact layer on the face of the cell where light enters is generally present in some grid pattern and is composed of a good conductor such as a metal. The grid pattern does not cover the entire face of the cell since grid materials, though good electrical conductors,

are generally not transparent to light. Hence, the grid pattern must be widely spaced to allow light to enter the solar cell but not to the extent that the electrical contact layer will have difficulty collecting the current produced by the cell. The back electrical contact layer has no such diametrically opposed restrictions. It need simply function as an electrical contact and thus covers the entire back surface of the cell structure. Because the back layer must be a very good electrical conductor, it is always made of metal.”

Although all solar cells operate on the same basic physics, there are differences in the semiconductor materials used. Some early cells, for instance, used indium phosphide (InP) as the photovoltaic material. Most satellites launched in the past decade have used various types of silicon (Si) cells, although gallium arsenide (GaAs) gained favor in the past five years or so. Now, multijunction cells that combine layers of various types of materials are being mass-produced and launched on commercial spacecraft.

1. Silicon Solar Cells

Every silicon atom has four valence electrons which are typically shared with adjacent silicon atoms in covalent bonding. Such a silicon crystal can be doped with an impurity such as phosphorus which has five valence electrons. This “extra” electron is then basically free to wander about the crystal lattice. This is the basis of an N-type semiconductor.

If the crystal is doped with boron, for instance, which has three valence electrons, holes are created which results in a P-type (positive-type) material. The essence of photovoltaics is that if light of an energy level greater than the band gap of the material falls upon the crystal, it will excite a valence electron leaving a hole. Under the influence of an electric field, these electrons are driven toward a lower energy state in the n-type material while the holes move toward a lower energy state in the P-type side. (Merrigan, p.30-32)

This is inherently not a 100% efficient process. First, only the light whose energy is higher than the band gap of the material will produce photocharges. Some light is reflected off the surface of the material, which is accounted for using the reflectivity, R . Applying antireflective coatings that have indexes of refraction somewhere between those of the semiconductor and air can reduce these reflections. (Hu, p.82)

Also, each photon having $h\nu > E_g$ can generate one and only one electron-hole pair; any excess energy is dissipated as heat. (Hu, p.44) Added to this, only a fraction of the possible light is actually absorbed in the crystal. The following equation dictates that fraction, where α is the absorptivity and th is the thickness of the material. (Merrigan, p. 34)

$$F.A. = 1 - e^{-\alpha h}$$

Even so, another clever technique involves plating the back surface of the cell with highly reflective materials, thus making the light make two passes through the cell. (Hu, p. 227)

Seale gives an outstanding description of the various types of Si solar cell technology when he explains, “The most common material used in solar cells is single crystal silicon. Solar cells made from single crystal silicon are currently limited to about 25% efficiency because they are most sensitive to infrared light, and radiation in this region of the electromagnetic spectrum is relatively low in energy.” An example of single crystal solar cells is shown in Figure 5.2.

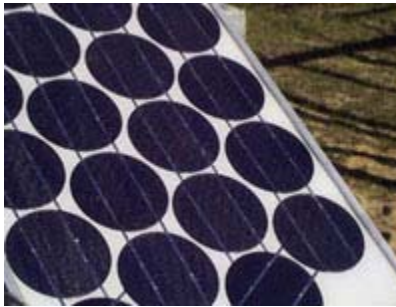


Figure 5.2 Single Crystal Solar Cells (image courtesy ACRE)

But single crystal silicon isn't the only material used to build solar cells. Polycrystalline ("many crystals") solar cells (Figure 5.3) are made by a casting process in which molten silicon is poured into a mould and allowed to cool, then sliced into wafers. This process results in cells that are significantly cheaper to produce than single crystal cells, but whose efficiency is limited to less than 20% due to internal resistance at the boundaries of the silicon crystals.

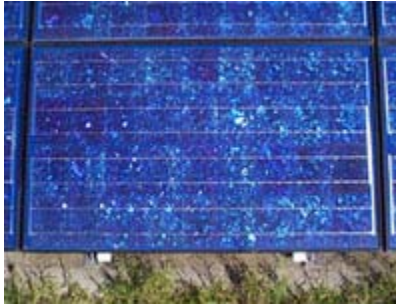


Figure 5.3 Polycrystalline Solar Cells (image courtesy ACRE)

Amorphous cells (Figure 5.4) are made by depositing silicon onto a glass substrate from a reactive gas such as silane (SiH_4). This type of solar cell can be applied as a thin film to low cost substrates such as glass or plastic. Thin film cells have a number of advantages, including easier deposition and assembly, the ability to be deposited on inexpensive substrates, the ease of mass production, and the high suitability to large applications. Since amorphous silicon cells have no crystal structure at all, their efficiencies are presently only about 10% due to significant internal energy losses.”



Figure 5.4 Amorphous Solar Cells (image courtesy ACRE)

Silicon's band gap is 1.10 eV. Photons of energy less than that will not create an electron-hole pair. For monochromatic illumination, that corresponds to a light wavelength of less than around 1.13 μm . DF and CO_2 lasers will produce no output from a silicon photovoltaic cell.

The fairly low efficiencies of silicon solar cells are offset by their extremely low cost for many terrestrial applications. However, as spacecraft have grown in complexity and hence in their power demands, there is a need for more sophisticated materials.

2. Gallium Arsenide Solar Cells

GaAs has been under development as a photovoltaic material since the mid-1950's. Early on, it demonstrated the potential for high efficiency, low performance degradation with increased temperature, and tolerance to total dose ionizing radiation. (Mazer, p. 178)

The Department of Energy reports that "Gallium arsenide (GaAs) is a compound semiconductor: a mixture of two elements, gallium (Ga) and arsenic (As). Gallium is a byproduct of the smelting of other metals, notably aluminum and zinc, and it is rarer than gold. Arsenic is not rare, but it is poisonous. Gallium arsenide's use in solar cells has been developing synergistically with its use in light-emitting diodes, lasers, and other optoelectronic devices.

GaAs is especially suitable for use in multijunction and high-efficiency solar cells for several reasons: The GaAs band gap is 1.43 eV, nearly ideal for single-junction solar cells; GaAs has an absorptivity so high it requires a cell only a few microns thick to absorb sunlight (Crystalline silicon requires a layer 100 microns or more in thickness.); Unlike silicon cells, GaAs cells are relatively insensitive to heat (Cell temperatures can often be quite high, especially in concentrator applications.); Alloys made from GaAs using aluminum, phosphorus, antimony, or indium have characteristics complementary to those of gallium arsenide, allowing great flexibility in cell design; and GaAs is very resistant to radiation damage. This, along with its high efficiency, makes GaAs very desirable for space applications.

One of the greatest advantages of gallium arsenide and its alloys as PV cell materials is the wide range of design options possible. A cell with a GaAs base can have several layers of slightly different compositions that allow a cell designer to precisely control the generation and collection of electrons and holes. (To accomplish the same thing, silicon cells have been limited to variations in the level of doping.) This degree of control allows cell designers to push efficiencies closer and closer to theoretical levels. For example, one of the most common GaAs cell structures uses a very thin window

layer of aluminum gallium arsenide. This thin layer allows electrons and holes to be created close to the electric field at the junction.”

The band gap of GaAs is 1.42 eV, corresponding to a monochromatic wavelength of less than around 877 nm. Longer wavelengths do not have the necessary energy to generate electron-hole pairs. In addition to the lasers that do not generate electricity in silicon cells, the ubiquitous Nd:YAG is of no use with GaAs.

3. Multijunction Solar Cells

Merrigan, made the claim in 1975 that, “It is not expected that the efficiency of photovoltaic energy conversion at ambient temperatures will ever exceed 25%.” He has been proven wrong.

Reinhardt reports that AFRL has already developed 25% efficient solar cells, using a multi-junction design. In multi-junction cells (shown in Figure 5.5), various layers of different materials are grown or bonded together. Each material has a different band-gap, meaning that it takes light of different energy levels to create electron-hole pairs. In general, low band-gap materials are placed at the top of the cell, since higher energy photons can pass right through. Through clever manipulation of the cell materials, composition, and thicknesses scientists have been able to exhibit conversion efficiencies unheard of in single-layer photovoltaics.

Reinhardt’s report projects that the majority of the 800 estimated military and commercial space systems to be developed over the next five years will use multi-junction cells. Since cell efficiency has been increased by at least 35% and the program limited the cost increase to only 15% over that of single-layer cells, there is a resultant reduction of 15% in cost per watt. The cells use legacy substrate materials, meaning there is no additional cost or complexity to spacecraft designers when switching from traditional single-layer cells. The higher efficiency allows higher power missions or lighter-weight power collection systems, leading to increased mass available for payload design.

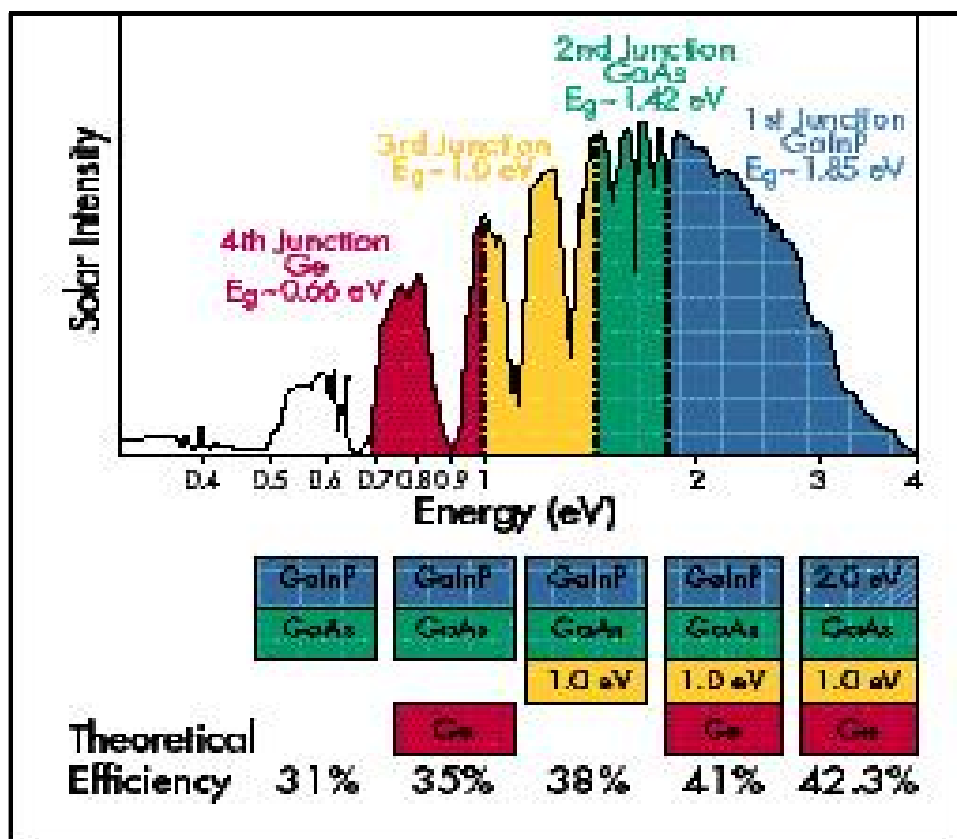


Figure 5.5 Multijunction Cell Materials and Solar Illumination

Already Reinhardt's group at AFRL has designed a four-junction cell that is projected to have a conversion efficiency of 35% to 40%. Their history and future projections are shown in Figure 5.6.

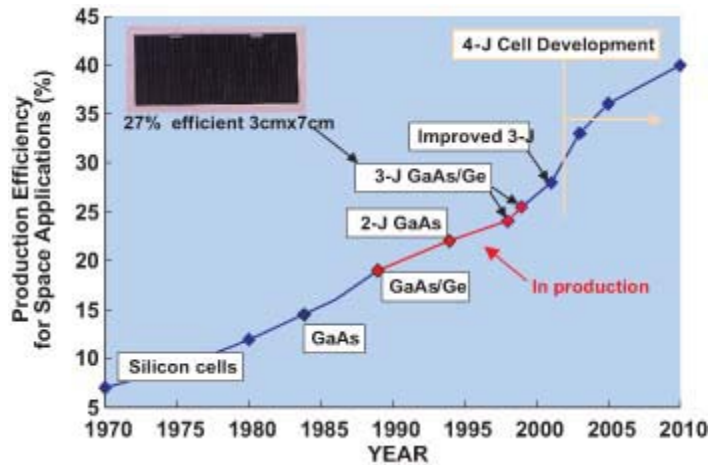


Figure 5.6 Trends in Air Force-Funded Space Solar Cell Development

Unfortunately, multi-junction solar cells are not good candidates for laser power beaming, at least not without some modification of the concept of operations. Because the various photovoltaic materials are mated in a series fashion, the current output of the cell is limited to the lowest current produced by any of the layers. Monochromatic light from a laser has the potential to generate a large current in the one layer whose band-gap is closest to the laser wavelength, but the overall output of the cell will be zero. For future power beaming applications, therefore, multiple laser sources would have to be used at the same time, each one corresponding to a highly efficient peak in response for a particular layer in the cell.

B. PHOTOVOLTAIC POWER CONVERSION OF LASER ENERGY

Sandia and NASA have done other studies into photovoltaic energy transfer of beamed laser energy. Current satellites predominantly use silicon (Si) or gallium arsenide (GaAs) solar cells which exhibit peak efficiency to light at 950 nm and 850 nm respectively. They have found that solar cells' response to monochromatic light near these optimum wavelengths is roughly double that produced by sunlight. Monroe conservatively calculates that the equivalent of one sun of illumination would require 915 W/m² of 850 nm light. Michael puts the figure at closer to 700 W/m². In any event, a 100 kW laser with realistic-sized adaptive optics can easily produce one or more suns of illumination. Some current HELs operate at 530 nm, the wavelength of a frequency-

doubled Nd:YAG laser. Landis reveals that the atmosphere transmits 67% of the energy at this wavelength and that GaAs operates at 25% efficiency at 530 nm. One sun of illumination at that wavelength still only requires around a megawatt of laser output.

Looking even further into the future, Sandia and NASA have independently proposed 200 kW solutions. In each case, an array of lasers is coherently fused to produce the high-energy beam. These systems would produce 3 kW/m² at the satellite, essentially quadrupling the power output of the solar arrays.

NASA has also poured much time and effort into their Space Solar Power program, a novel effort to collect solar energy in space and transmit that power to ground stations. As far back as 1990, Williams published that, “The basic idea is to use a power source (e.g. nuclear or solar) to generate a powerful laser beam and transmit the beam, collimated and focused, to user locations where its power can be used as is or converted to other forms such as electrical or thermal power.” NASA’s Wireless Power Transmission working group is currently debating whether laser or microwave radiation is the best way to transmit power once it is collected in space; each approach has its benefits and limitations.

Some scientists have looked at novel ways to convert laser energy to spacecraft power *without* using photovoltaics. DeYoung proposed some interesting optical rectification, laser-driven magnetohydrodynamic, and reverse free-electron laser concepts, and Michael described the use of thermophotovoltaics which actually rely on the generation of heat rather than the absorption of photons to create electricity. Still, these ideas are unproven advanced concepts which will require decades of research before they can be used in practical applications. For current and near-term solutions, photovoltaic cells are the clear choice.

VI. ANNEALING OF RADIATION-DAMAGED SOLAR CELLS

A. RADIATION DAMAGE

Space is a harsh environment. All kinds of radiation bombard objects in space orbit, and the solar cell units, which by design have a large cross-sectional area, absorb lots of it. All damage from radiation is standardized in units called the “normally incident damage equivalent 1-MeV fluence.” (Rauschenbach, p. 2.5-2) This quantifies the effects of incident electrons, protons, neutrons, gamma rays, alpha particles, etc. into a single standardized unit for comparison.

The various types of radiation can cause different kinds of damage to the sensitive solar cell material. Chase explains that ionization damage removes orbital electrons, changing the majority and minority carrier concentrations within the cell. Displacement damage occurs when atoms are actually bumped out of their spots in the crystal lattice, leaving a vacancy and normally finding another semi-stable position in the lattice called an interstitial. (p. 35) Both of these forms of damage serve to reduce the voltage or current produced by the cell, resulting in lowered power output.

As time goes on, the effects of ionization damage and displacement damage compound. Solar cell coverglass is darkened, resulting in lowered transmissivity. Vacancy/interstitial pairs (called Frenkel pairs) are referred to as recombination or trapping sites since they “are responsible for trapping a charge carrier and allowing another charge carrier to recombine with it neutralizing both charges.” (Chase, p. 37)

The result of this damage is the addition of new allowed energy states within the energy bandgap. As Chase describes on page 42, these additional energy levels change the electrical properties of the p-n junction device through mechanisms called “carrier trapping, dopant compensation, electron-hole pair recombination, thermal generation of electron-hole pairs, and tunneling.” Every one of these mechanisms serves to reduce the power output of the cell, either by dropping the short circuit current, open circuit voltage, and ultimately maximum power output or efficiency. (Chase, p. 47)

Radiation degradation of solar array output is one of the most critical limiting factors on the lifetime of a satellite. Especially for geosynchronous communications

satellites, a certain amount of power must be generated at all times to power traveling wave tube amplifiers (TWTAs) and bus components. When the satellite can no longer meet this minimum power requirement when eclipsed, the satellite is basically shut down. A half-billion dollar investment which might be usable 95% of the time becomes space junk. If there was a reliable way to repair this damage while a spacecraft remained on-orbit, it could literally save billions of dollars.

B. ANNEALING METHODS

There are two basic methods for annealing radiation damage in solar cells. The first, thermal annealing, is similar to the process used for correcting materials deficiencies in metals. The second is current annealing, which involves the application of large electrical flows into the material.

In either method, the increase in energy excites substrate electrons which moves them into new positions within the atomic structure. The crystal lattice is restored almost to original conditions when the excited electrons fill holes which were created by the damaging irradiation. (Michael, p. 1178)

1. Thermal Annealing

Thermal annealing in the traditional sense requires a metal to be heated to several hundreds of degrees centigrade. These high temperatures would destroy the relatively delicate structure of a semiconductor, so thermal annealing of solar cells takes place at much lower temperatures, on the order of 20° C to 50° C.

Michael's paper describes both periodic thermal annealing, where the cell is isothermally annealed at a specified temperature for a short period of time, and continuous annealing when the cell is annealed at the same time as it is exposed to damaging radiation. (p. 1178)

Thermal annealing has extremely limited utility for solar cells in space. Achieving the temperatures required is quite difficult, especially when the cells are not directly illuminated by the sun. Also, annealing at lower temperatures takes a very long time, making current annealing a much more attractive option.

2. Current Annealing

Michael's paper explains, "Minority carrier injection annealing is the application of a forward bias current to the cell's junction." (p. 1179) There are two methods of achieving minority carrier injection: photoinjection (the surface of the cell is illuminated with a high-intensity light source) and forward bias injection (electric potential is forced across the cell in the forward direction, increasing the current exponentially and the dissipated power proportionally).

NPS research conducted by Cypranowski conclusively demonstrated that low-temperature minority carrier annealing of both GaAs and InP cells significantly recovered radiation-degraded parameters. Although this particular study used forward bias injection, subsequent research has demonstrated photoinjection annealing using laser light.

Groundbreaking work in this area was performed by Chase in 1995. He described why thermal annealing was infeasible for solar cells, and why forward-biased current annealing is only feasible for future spacecraft that are designed with this capability in mind. (p. 57) His thesis work focused on using lasers for photoinjection annealing of indium phosphide solar cells.

Solar cells are significantly more efficient to monochromatic light than to broadband light such as that produced by the sun. Each solar cell material has a peak response to light at a specific wavelength which corresponds to the energy bandgap of the material. As described in the previous chapter, light at longer wavelengths (lesser energy) cannot create an electron-hole pair; it simply heats the cell, which will itself reduce efficiency. Elimination of these photons using a monochromatic source is another source of increased cell efficiency.

Chase's work involved irradiating his test InP cells using the NPS linear accelerator. He measured a baseline I-V curve for two cells, degraded them to a fluence level of 1×10^{15} electrons/cm², and then measured the cell response (I-V curve). He then annealed them in a test cell at 48.5° C using an 8 W argon ion laser whose primary transmission lines are at 488 nm and 514 nm. He estimated the power density striking the cell at 2.5 W/cm². The lasing took place for one hour, and in the second test for

fifteen minutes. He then obtained I-V curves for the cells to determine how much of the lost efficiency was regained through annealing.

The results showed a 17% gain in efficiency for one cell and 18.7% for the other which, while significant, were not as high as expected. For his next set of tests, he irradiated them less and annealed at higher temperatures. At 60° C and lased for fifteen minutes, the cell regained 48% of its lost efficiency. A final test at 75° C resulted in only a 21.2% recovery.

Chase identified several issues in the execution of his tests, including uncertainties in laser output, non-optimal irradiation levels, cell material problems, etc. Still, the results clearly show that laser annealing is a reality and that it can be optimized based on the cell material, amount of damage incurred, temperature, and other factors.

3. Conclusion

Annealing is not solely an artificially-imposed effect. In fact, Mazer reports that, “When deployed in space, n+p InP cells experience both thermal annealing and radiation-induced annealing. That is, the radiation resistance is improved while the cells are illuminated.” (p. 188)

C. MEASURING CELL OUTPUT

Every solar cell’s performance can be described by using an I-V curve. These curves graphically demonstrate the output of a particular cell under varying conditions, and are generated by connecting the cell to a specially designed circuit as shown in Figure 6.1 (Merrigan, p. 48):

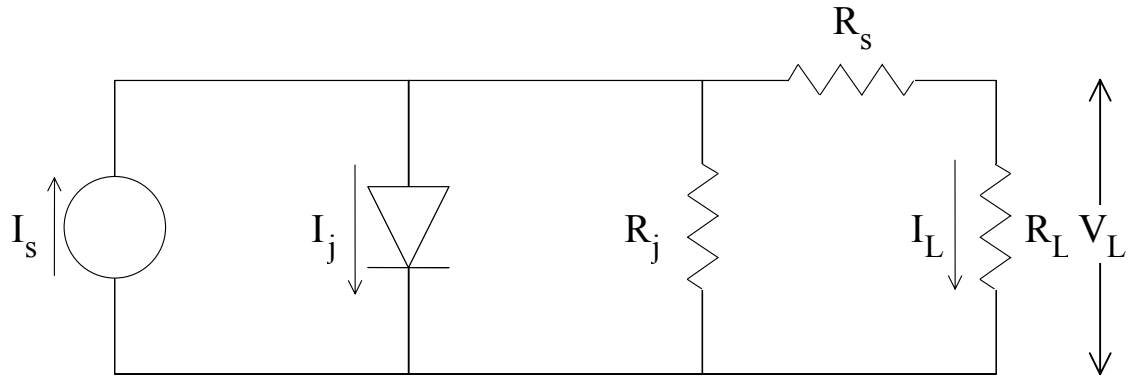


Figure 6.1 Circuit for Measuring Cell Characteristics

In this diagram, the following conventions are used:

- I_s : total separated charge
- I_j : current leaked across P-N junction
- I_L : load current
- R_j : junction resistance to leakage
- R_s : series resistance of cell
- R_L : load resistance
- V_L : load (cell) voltage

Two of the critical cell parameters are the open circuit voltage (V_{OC}) and the short circuit current (I_{SC}). V_{OC} is measured when $R_L = \infty$, and I_{SC} is measured when $R_L = 0$. As the load resistance is varied, the output voltage and current are measured, generating a curve between the two points. The knee of the curve represents the maximum power point for the cell—the place where the current times the voltage reaches its highest value. An example of an I-V curve with each of these points of interest pointed out is shown in Figure 6.2.

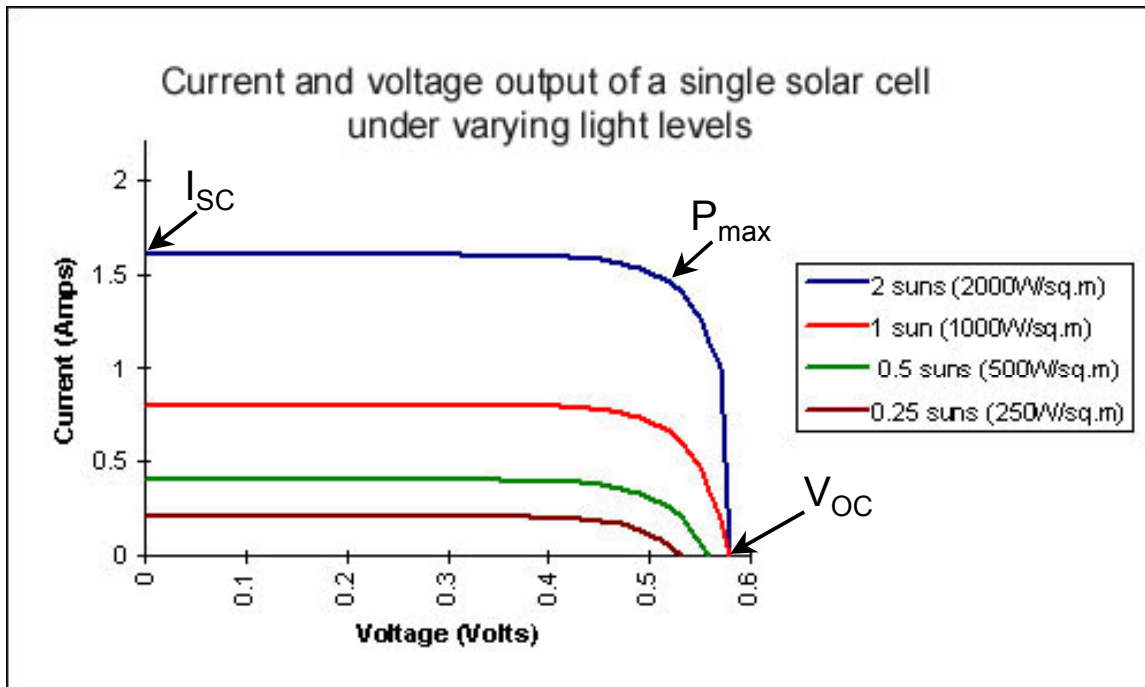


Figure 6.2 Solar Cell I-V Curves (Carr)

Measuring the output of multi-junction cells introduces additional challenges. Sandia National Laboratories is a leader in characterizing these new cells, and has developed the most advanced simulation and testing methodology available. They have developed a proprietary software package called IV Tracer that contains a database of single junction and multi-junction cell performance parameters and models. The Maui Solar Energy Software Corporation helped develop this tool, which enables cell designers and users to estimate the performance of various types and configurations of cell arrays.

Sandia also has extensive laboratory facilities that enable “current-voltage measurements in forward and reverse bias using a xenon-arc solar simulator, absolute spectral response measurements of separate junctions using both light and voltage bias, a device simulation model, and a spectral mismatch calculation procedure tailored to multi-junction cells.” (King, p. 1)

When trying to measure the benefits gleaned from annealing, it is useful to consider that “the primary effect of radiation defects to a crystal lattice is the reduction in minority carrier diffusion lengths or lifetimes.” (Chase, p. 51) Chase goes on to explain that the recombination rate is inversely proportional to the minority carrier lifetime.

There is a relationship between the change in recombination rate of a radiation-damaged cell to an undamaged one plus the rate due to radiation fluence levels. It turns out that the real world is not so straightforward, as minority carrier lifetimes are too short to be physically measured; instead, the cell's electrical properties (which can and often are recorded) are used.

THIS PAGE INTENTIONALLY LEFT BLANK

VII. GROUND AND ON-ORBIT TESTING

A. THE PETITE AMATEUR NAVY SATELLITE (PANSAT)

1. PANSAT Overview

PANSAT is “a proof of concept, half-duplex, digital spread-spectrum, store-and-forward communications satellite” that was designed by students, faculty and staff at NPS. “The spacecraft itself provides store-and-forward (packet radio) digital communications using direct sequence spread spectrum modulation. PANSAT operates in the amateur radio 70 cm band with center frequency at 436.5 MHz, a bit rate of 9842 bits per second and 9 MB of message storage. Amateur radio ground stations will be able to utilize PANSAT via a bulletin-board type user interface.” (Sakoda)

Peat’s excellent website reveals that PANSAT’s NORAD 2-line element set number is 25520, and its international designation code is 1998-064-B. It was launched by the Space Shuttle Discovery (STS-95, the John Glenn mission) at 19:19 UTC on 29 Oct 98. The two-line orbital elements for PANSAT are:

```
1 25520U 98064B 02324.75462098 +.00004483 +00000-0 +23501-3 0 06207
2 25520 028.4606 101.8358 0006091 101.0293 259.1013 15.13284031223961
```

Table 7.1 is a representative set of orbital elements for PANSAT, while Figure 7.1 illustrates a representative PANSAT ground trace:

Epoch (UTC):	6:06:39 PM, Wednesday, November 20, 2002
Eccentricity:	0.0006091
Inclination:	028.4606°
Perigee Height:	522 km
Apogee Height:	530 km
Right Ascension of Ascending Node:	101.8358°
Argument of Perigee:	101.0293°
Revolutions per Day:	15.13284031
Mean Anomaly at Epoch:	259.1013°
Orbit Number at Epoch:	22396

Table 7.1 PANSAT Orbital Elements

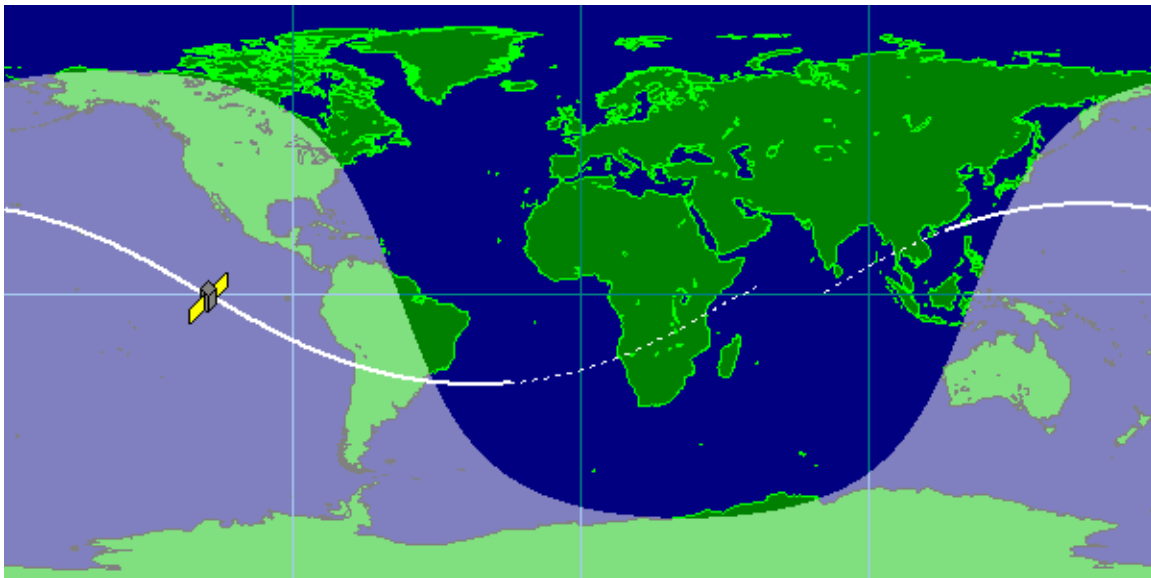


Figure 7.1 PANSAT Ground Trace (Peat)

PANSAT is made up of eighteen square and eight triangular aluminum panels. Seventeen of the panels are covered with silicon solar cells, and the one panel containing the launch vehicle interface (spring-launch mechanism for deploying the spacecraft from the GAS can in the Shuttle) has a circular gallium arsenide cell. (Bible) The spacecraft is

approximately 19 inches in diameter and has no attitude control or propulsion system. The only spacecraft subsystems are the communications payload, the electrical power subsystem (solar cells, batteries, and distribution/regulation equipment), and the digital control subsystem. (Sakoda) Figure 7.2 illustrates the locations of the various solar cells and their nomenclature.

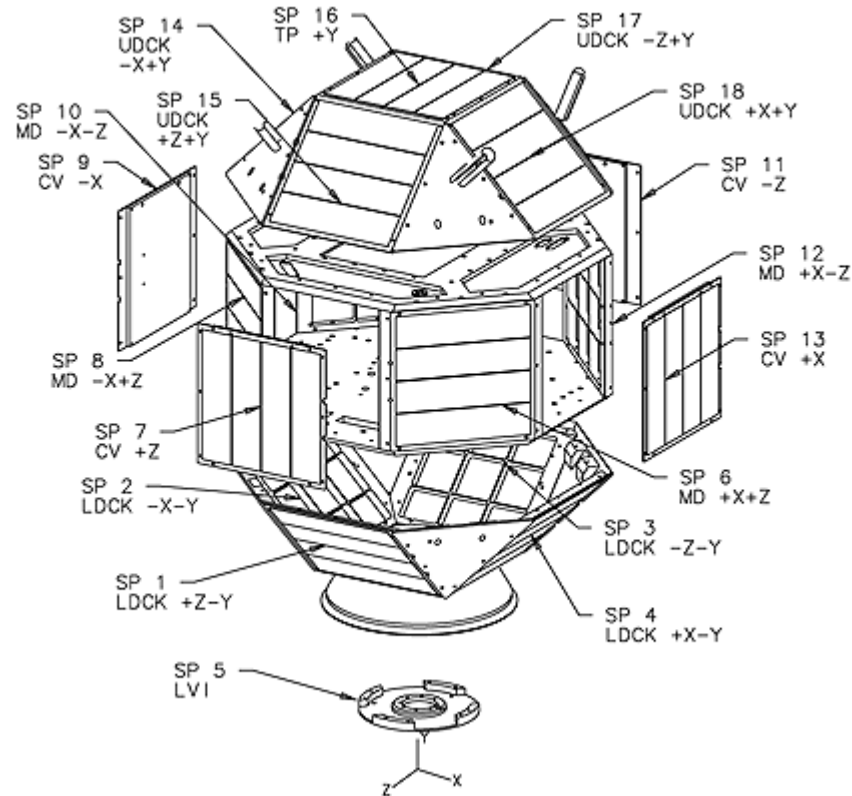


Figure 7.2 PANSAT Solar Panel Identification (Sakoda)

Power is stored in two batteries, each of which consists of nine commercial NiCd cells. The Si cells are square 7" on a side, while the high-efficiency GaAs panel is circular with a diameter of 5.75". Figure 7.3 is an expanded view schematic diagram of the entire spacecraft.

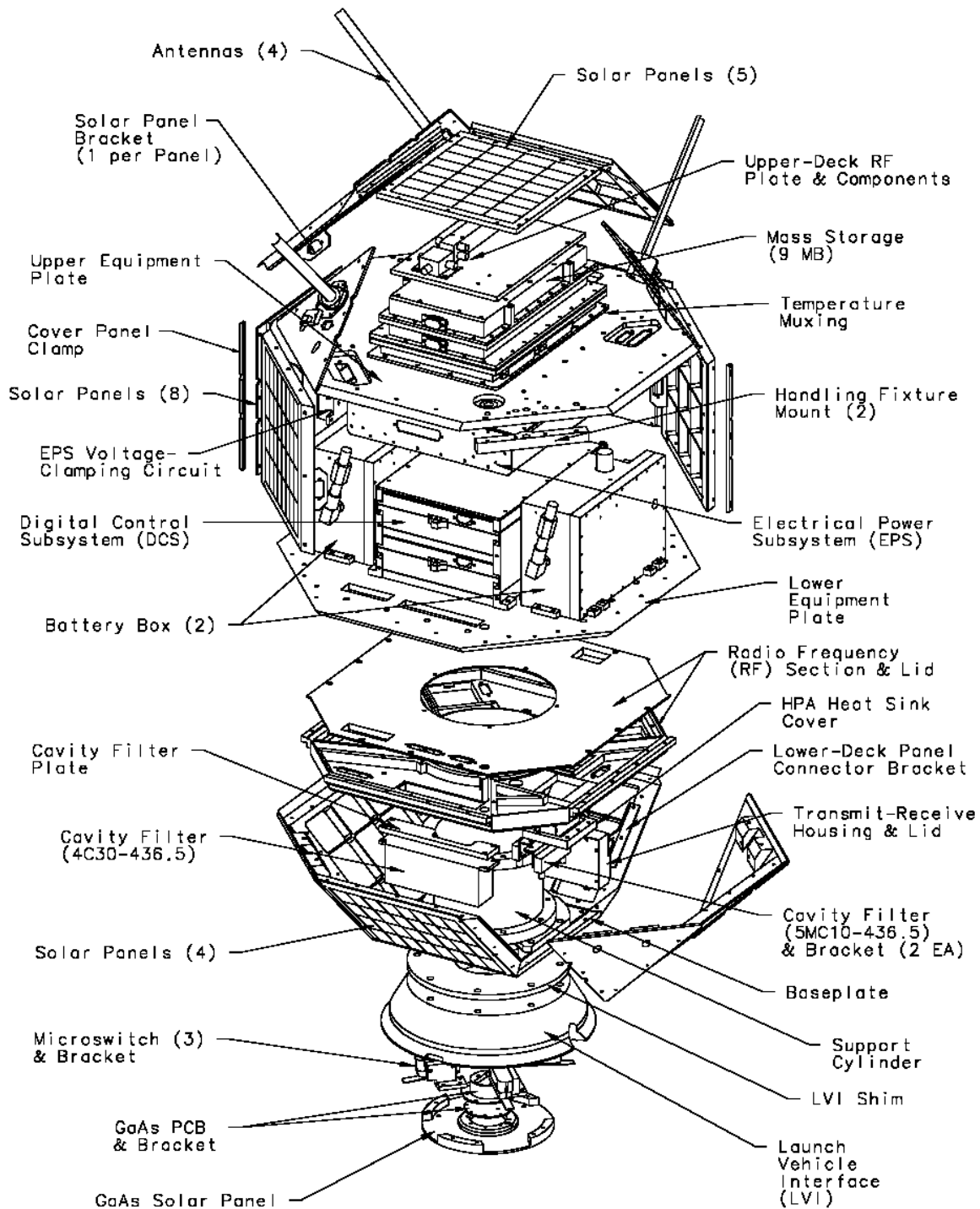


Figure 7.3 PANSAT Schematic Diagram (Sakoda)

Sakoda also posted the following picture of PANSAT (Figure 7.4) on his personal web page. It provides a good view of how the spacecraft actually looked when almost completed.



Figure 7.4 PANSAT Assembly Photo (Sakoda)

2. Suitability for On-Orbit Testing

PANSAT was chosen for on-orbit testing for a number of reasons. Although dozens of satellites were considered, PANSAT had a number of unique or desirable features that made it the proper choice.

Most satellite owners are reluctant (to say the least) to have high-energy lasers pointed at their valuable assets. Satellites which are past their end-of-life are not suitable

because there is no telemetry to measure the response of the satellite to lasing. So the best choices are those satellites that are operating near their end-of-life or past their design lifetime. Such assets have already “paid their dues”, and owning organizations are more open to scientific research that has the potential to damage their spacecraft. PANSAT was launched in October 1998 and had a two-year design life (with four to six years of operation considered a huge success). Rudy Panholzer, the chairman of the NPS Space Systems Academic Group and the controlling authority concerning PANSAT, enthusiastically supported this thesis experiment. His vision for PANSAT was that it would enhance student learning during design and operations, and the fact that it can continue to fulfill that role even after its design life is a bonus.

Due to the relatively low power of available laser sources, a satellite in LEO is far more attractive for this experiment than one in a higher altitude. Although a GEO or MEO spacecraft would make tracking easier and would also enable longer periods of lasing, diffraction of laser energy to that higher altitude greatly reduces the incident flux. PANSAT, at approximately 500 km altitude, is low enough to absorb a suitable amount of laser energy.

Since PANSAT was launched as a get-away special on the Space Shuttle, it is in a 28.5° inclined orbit. That means that it will, at some point in its orbit, pass directly overhead any site on the ground with latitude less than or equal to 28.5° . Figure 7.5 shows that only AMOS will get these 0° overhead passes. Even SOR, the second choice for a ground site, would be looking so far down on the horizon that it would be both difficult to track and would require additional laser power to burn through the extra atmosphere.

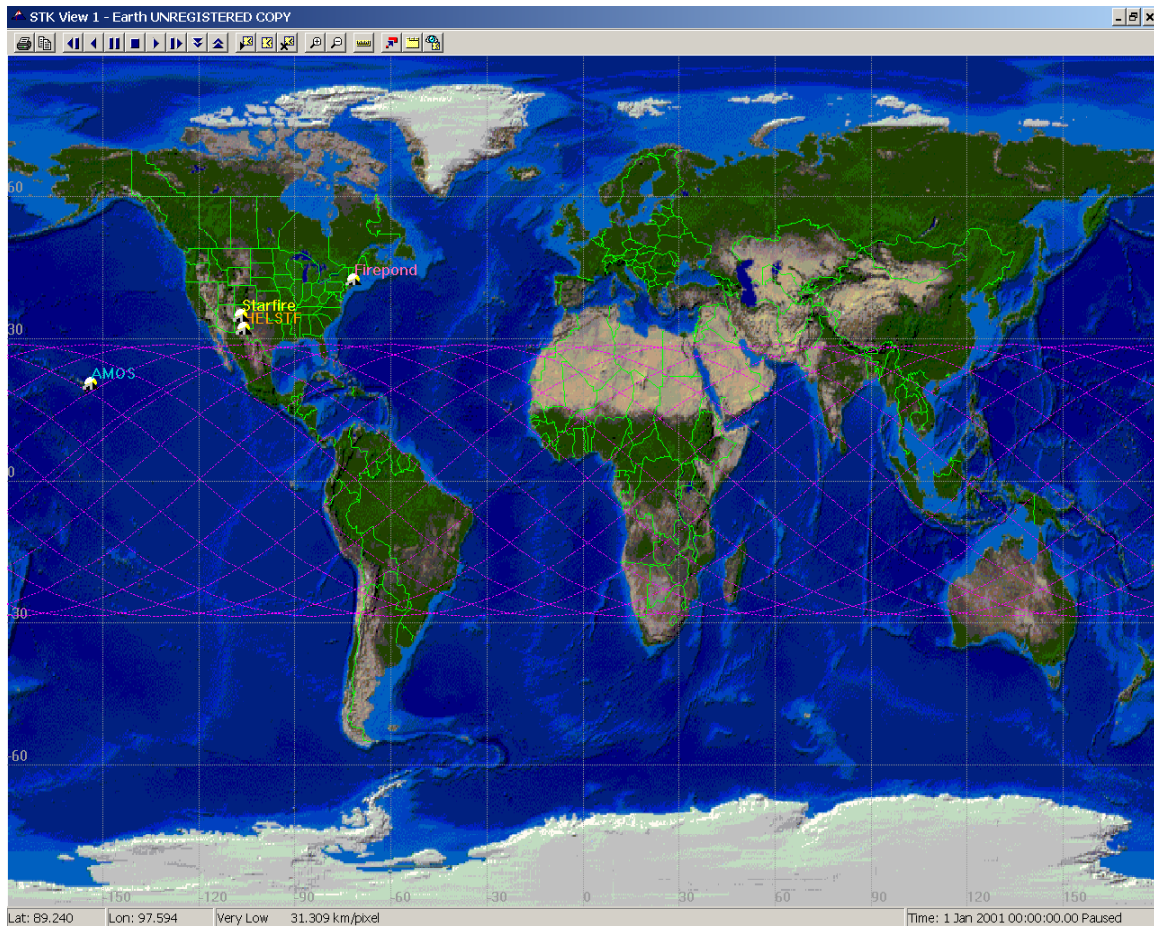


Figure 7.5 PANSAT and Ground-Based Laser Sites

In addition to technical considerations, AMOS is an attractive ground-based site for other reasons. AMOS, although it is an operational military facility, was designed with scientific research and academic projects in mind. The floor space under the 3.5 m AEOS telescope has several coudé rooms, and each one can be assigned to a specific research team. This allows multiple projects, sometimes at very different classification levels, to go on at once.

Another factor making PANSAT attractive for this test series is the fact that the satellite telemetry comes directly into a ground station at NPS in Monterey. That means that data is readily available, does not need to go through public release or classification review, and is in a well-understood format. Technicians at NPS constantly receive and evaluate PANSAT telemetry, creating historic trend charts like those in Figure 7.6.

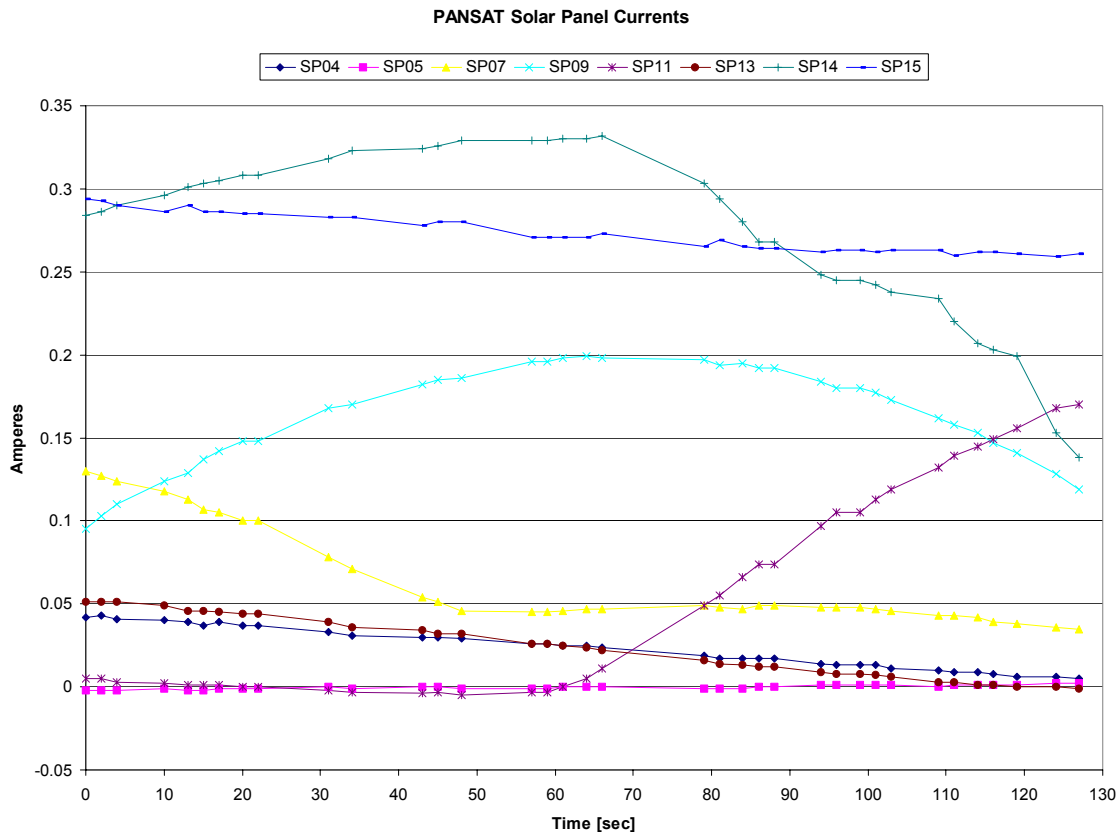


Figure 7.6 Example of PANSAT Solar Panel Telemetry

This particular chart shows the slow rotation of the spacecraft with respect to the sun. As panel SP14 rotates out of direct sunlight, SP11 is coming into view. This type of detailed data is essential to measuring the increased power output that would result from laser illumination. Since the laser would be illuminating earth-facing panels (which do not receive direct sunlight at the same time), it would be easy to identify increased current that is time-correlated with laser firing.

B. GROUND-BASED TESTING

Ground testing was completed at AMOS (Mount Haleakala, Maui) from 3-5 Dec 02. As mentioned previously, AMOS offered the most suitable combination of criteria that made it the test site of choice. Testing was accomplished using a NASA-provided IPG Photonics Model DLD-20 fiber laser (Figure 7.7) that operates at

975±5 nm at a rated power of up to 25 W. The laser was mounted on an optics bench in the Laser Beam Director (LBD) and all testing took place on the bench; no laser energy was propagated outside the building. This laser was used previously in NASA's wireless power transmission demonstration to a model lunar/Martian rover in the AMOS "doghouse".



Figure 7.7 Laser Used for Ground Testing

The first data collected was a solar illumination test of the extra PANSAT silicon solar panel which is maintained at NPS for such purposes. It is identical to the panels onboard the spacecraft but has been fitted by NPS technicians with power output connectors and a thermistor to measure the temperature of the panel. Although this test began at 1630 Hawaii time, the elevation of 10,000 feet above sea level makes the results comparable to those that would be obtained under AM0 solar conditions in space. The measured I_{SC} was 0.25 A and V_{OC} was 18.35 V. Efficiency for the panel was found to be

9.13%, assuming that a full 0.1352 W/cm^2 of solar illumination fell on the panel, as the measured peak power point produced an output of 3.362 W. The full I-V curve for the cell under solar illumination is shown in Figure 7.8 below:

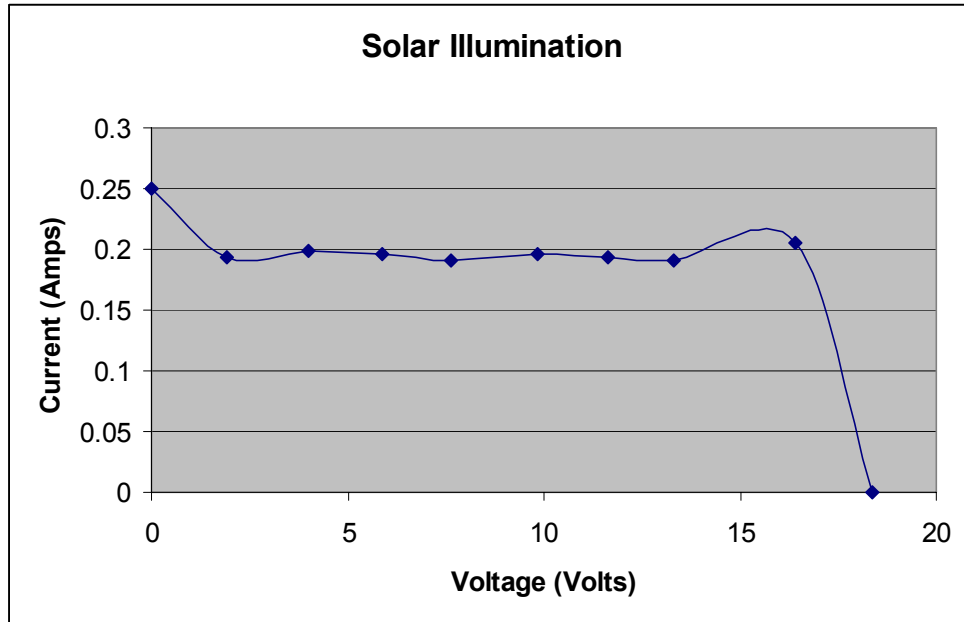


Figure 7.8 PANSAT Panel I-V Curve Under Solar Illumination

The next test attempted to project enough laser power onto the panel on the lab bench to match these solar illumination values. The distance from the laser source to the mounted PANSAT panel was estimated based on approximate beam divergence and trigonometry. The output of the laser diode diverges at a half-angle of approximately 10° , and a circular beam of diameter of at least 6.5 in was necessary to fully illuminate all cells in the panel. This necessarily led to some waste of the beam energy but gave an estimated distance of 21 in from the laser source. Starting with this value, the beam spread was measured using a phosphorescent card that glowed under near-IR illumination. Progressive measurements showed that the panel had to be mounted at a distance of 23 in in order to guarantee complete illumination. Figure 7.9 illustrates the lab bench setup used for these trials.

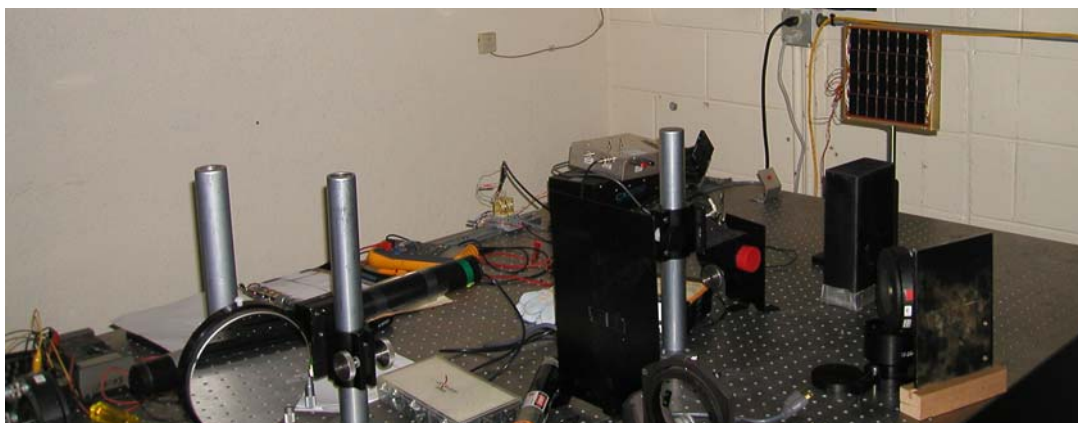


Figure 7.9 Lab Bench Setup

At that distance, it turned out that a laser output power of 7 W (as indicated by the internal electronic display on the laser) produced a V_{OC} of 18.5 V, close to the 18.35 V value obtained outside. I_{SC} under these conditions was 0.055 A. The maximum power point at the knee of the curve indicated an output of 0.9202 W for an overall system efficiency (including all the losses associated with not completely optimizing the laser beams spread onto the panel) of 13.1%. The thermistor indicated that the temperature of the cell was 22.5°C, up from the initial temperature of 20.1°C. The entire I-V curve is shown as Figure 7.10 below:

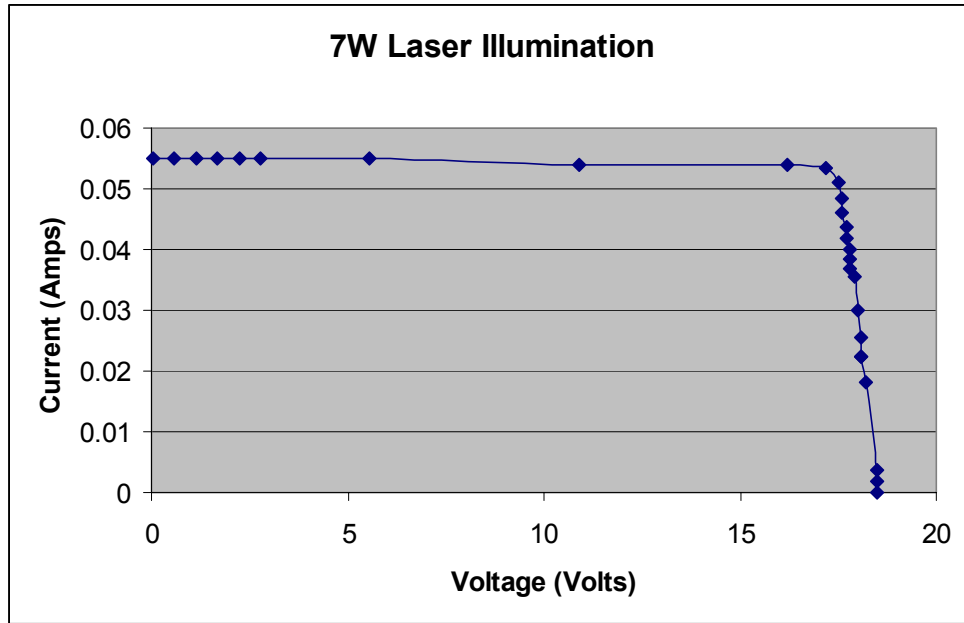


Figure 7.10 PANSAT Panel I-V Curve Under 7W Laser Illumination

The next set of tests ran the laser at 14W, double the output of the first test series. V_{OC} was now 18.9 V (up very slightly) and I_{SC} was 0.102 A (basically doubled). The maximum power point was 1.65 W for a system efficiency of 11.8%. The efficiency is likely dropping because the cell continued to heat up, now reaching a steady-state temperature of 27.5°C. Figure 7.11 below presents the overall I-V curve for this test:

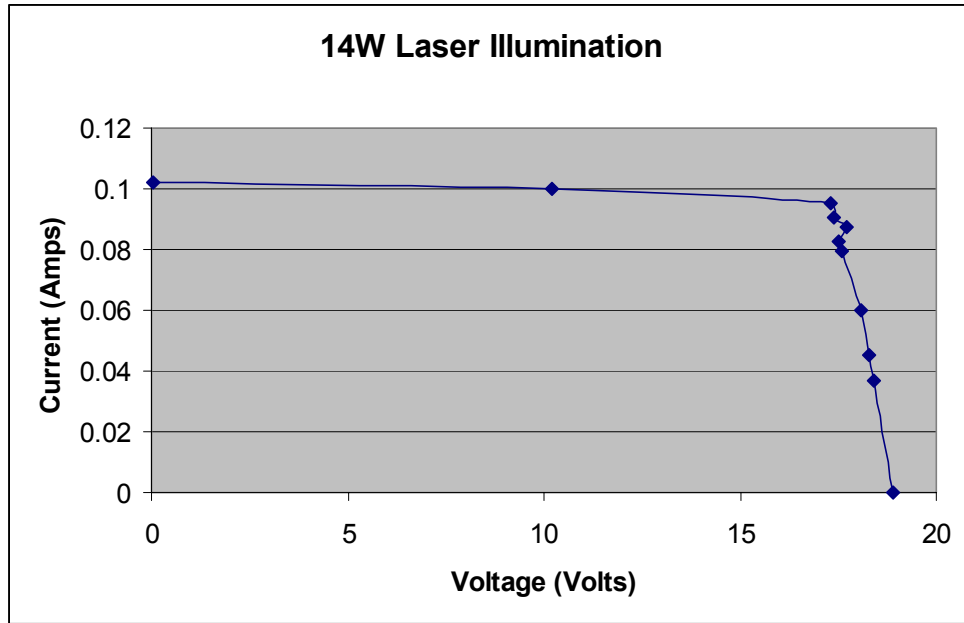


Figure 7.11 PANSAT Panel I-V Curve Under 14W Laser Illumination

The final set of laboratory tests involved turning the laser up to 21W, roughly triple the power of the initial test series. Now V_{OC} was 19.1 V (again up slightly), but I_{SC} rose to 0.151 A, as expected a tripling of the original output current. P_{max} was 2.38 W, revealing an overall system efficiency of 11.3%. Again the efficiency is lower, but this was to be expected as the panel temperature had now risen to 31.3°C, more than 11° higher than when testing began. Figure 7.12 below shows the overall I-V curve for this test series:

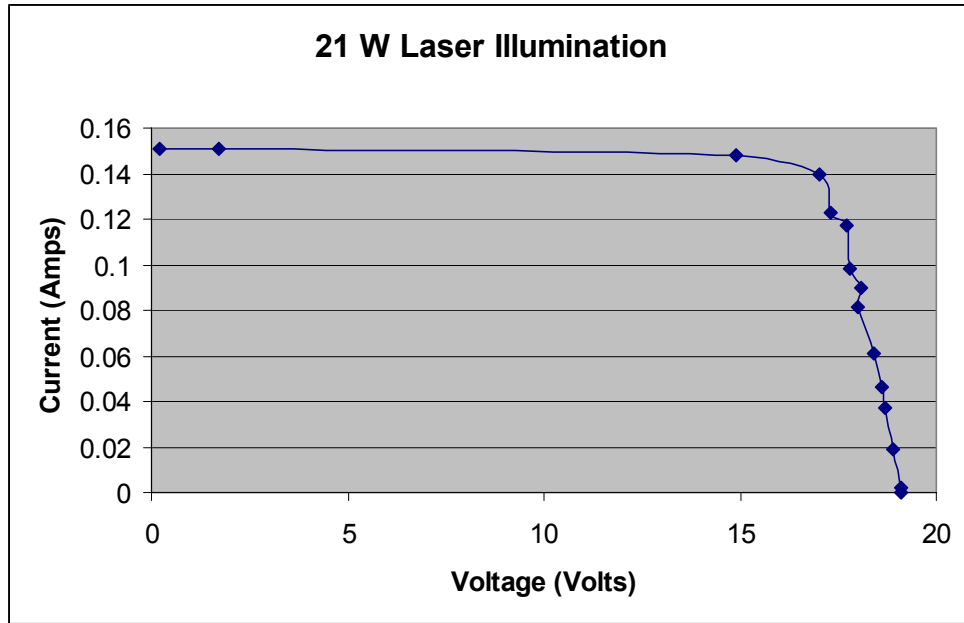


Figure 7.12 PANSAT Panel I-V Curve Under 21 W Laser Illumination

In addition to establishing a new baseline for the PANSAT silicon panels under AM0 solar illumination, these test series generated the first-ever hard data regarding the power output of the panel under 975 nm laser illumination.

	V _{OC} (volts)	I _{SC} (amps)	P _{max} (watts)	ε	T (°C)
AM0 solar	18.35	0.250	3.362	9.13%	20.1
7 W laser	18.5	0.055	0.920	13.1%	22.5
14 W laser	18.9	0.102	1.650	11.8%	27.5
21 W laser	19.1	0.151	2.380	11.3%	31.3

Table 7.2 Summary of PANSAT Panel Results

While Table 7.2 summarizes the key data collected during this series of experiments, it is important to keep in mind that the real goal is an on-orbit test, using a much higher-power ground-based laser to beam energy to PANSAT while it is in space.

C. ON-ORBIT TEST PLAN

If PANSAT is to be the target and Maui the ground site, what remains to be decided is what kind of laser to use. Bill Lowery, a Boeing employee who works at SOR, provided the equations for an initial analysis. He made clear that this is first-order, back-of-the-envelope work.

To estimate the irradiance at a target, start by calculating the angular spread of the beam. This is approximated by 2 times the wavelength over r_0 . A conservative value for Maui's r_0 is 20 cm, but it can be as good as 25 cm or even 30 cm. Then the beam spread is multiplied by the distance to the target (assuming 1,000 km for PANSAT, which is in a 555 km orbit but won't always pass directly overhead) to get the diameter of the beam at the target. From there it's easy to calculate the area of the beam, which is just divided into the output power to get irradiance.

Nominal solar irradiance is 1353 W/m^2 , but as stated earlier solar cells are more responsive to certain colors of monochromatic light than they are to the entire solar spectrum. It is assumed that the silicon cells on PANSAT are operating at about 10% efficiency right now after four years of operation. Silicon is about 20% efficient at 532 nm, 40% efficient at 850 nm, and roughly 15% efficient at 1.064 μm .

One sun of laser illumination would be great, but is perhaps impractical at this point. A quarter sun and a tenth sun at the satellite are more easily achievable. Given the PANSAT telemetry data, confidence is high that a quarter sun illumination would show up clearly on the dark panels. A tenth sun should show up, but increases the risk in the testing process.

The results of this analysis are shown below in Table 7.3:

Wavelength	$1/4$ Sun Illumination	$1/10$ Sun Illumination
532 nm	500 W	200 W
850 nm	750 W	300 W
1.06 μm	2 kW	800 W

Table 7.3 Required Laser Power Levels

Nd:YAG would be the easiest to obtain, even at a kilowatt or so, but prices, reliability, and beam quality need to be considered. If it fit into the future experimental budget and one could be obtained that operates in either fundamental or frequency-doubled mode that would be ideal. A hefty diode laser around 850 nm would also be rather interesting, and maybe the best choice overall.

Once a suitable laser source is procured and installed at AMOS, the next step would be to let the on-site orbital analysts develop a list of suitable passes for illumination. This is done by considering orbital dynamics and fly-over times of the satellite, predictive avoidance in consultation with the Laser Clearinghouse at Cheyenne Mountain, site availability, and other factors. Some passes directly overhead (elevation angle of 90°) are desirable, as are others lower towards the horizon. The overhead passes will allow for maximum laser flux while longer slant ranges can be used to determine the effects of atmospheric transmission and diffraction.

As of the time of writing this thesis, some problems with PANSAT's power system have developed that may substantially affect any on-orbit experiment. PANSAT's batteries have started to fail, leaving it unpowered during eclipse. Every orbit, when it passes into darkness, the satellite's systems shut down and then restart once the solar cells are illuminated. In addition, the receiving antenna is suffering increased losses leading to reduced command transmission rates.

The impact of these degradations is that telemetry data, which used to be "stored and forwarded" to the PANSAT ground site in Monterey is now only transmitted when the satellite is in sunlight and within range of the ground antenna. Telemetry from other parts of the orbit is lost. In addition, no commanding other than the nominal telemetry mode is possible. For example, ground controllers used to be able to upload a program which would command the spacecraft to take telemetry snapshots at short time intervals. This can now only be commanded in near-real-time, meaning that the ground controller sends a command asking for a telemetry readout. It takes a few seconds for the command to transfer and be understood, then for the data to reach the ground, so at best this will give a data resolution of one sample every seven seconds or so.

The indirect impact of this is that it limits the data collection possibilities tremendously. The few passes that the AMOS orbital analyst finds suitable will be

further winnowed by looking at only those passes where PANSAT will be in the sun's illumination over both Maui and Monterey. This would be perhaps too stringent a limitation.

For proper on-orbit testing, therefore, the PANSAT ground station should be temporarily moved to Maui. The equipment needed to do this, while bulky, can be carried by a team of three or four people on commercial aircraft. The PANSAT ground controllers should deploy with the equipment, both to set it up and monitor PANSAT during the test, but also to help with data acquisition issues.

THIS PAGE INTENTIONALLY LEFT BLANK

VIII. CONCLUSION AND RECOMMENDATIONS

This thesis pulled together concepts and background on lasers, electric propulsion, photovoltaic technology, and damage annealing. It describes an experiment at AMOS which provides a baseline of solar and laser illumination data for the silicon solar panels on PANSAT. It also develops a test plan for future a future on-orbit experiment which will further extend the results and come even closer to demonstrating an operational power beaming system.

Ground-based laser illumination of the PANSAT silicon solar cell array demonstrated the potential of power beaming to this asset. The on-orbit test using PANSAT will serve as a proof-of-concept of the feasibility of using high-energy lasers to both anneal radiation-damaged photovoltaic cells and to beam power to operational spacecraft. As higher-energy lasers become more readily available, it will become easier to conduct further demonstrations. Once word spreads that this technology is widely and affordably available, spacecraft designers will be able to take these concepts into account, creating vastly more efficient satellites with far longer design lifetimes.

When power subsystems are no longer a primary limiting factor in end-of-life considerations, spacecraft systems engineers will be able to shift their focus to other critical areas. In addition, as the weight and complexity of the power subsystem decreases, it will enable the use of lighter launch vehicles or allow larger payloads to be used with similar buses.

For the first time in almost fifty years, a revolution in satellite design is upon us. Robert Goddard, the famous rocket pioneer from my hometown of Auburn, MA, summed it up well when he said, “It is difficult to say what is impossible, for the dream of yesterday is the hope of today and the reality of tomorrow.”

THIS PAGE INTENTIONALLY LEFT BLANK

LIST OF REFERENCES

- ABL Homepage. <http://www.airbornelaser.com/>. October 2001.
- ACC/DR. "Airborne Laser", <http://xr.acc.af.mil/worldaccess/Staff/abl/abl.htm>. October 2001.
- "AMOS Maui Space Surveillance System", <http://ulua.mhpcc.af.mil/AMOS/mission.html>. June 2002.
- AMOS Users' Manual. <http://ulua.mhpcc.af.mil/AMOS/manual.html>. June 2002.
- Bamberger, Judith A. and Edmund P. Coomes. "Power Beaming Providing a Space Power Infrastructure", IEEE AES Systems Magazine, November 1992.
- Bennett, Hal E. "DoD and Navy Applications for Laser Power Beaming", SPIE Laser Power Beaming II Proceedings, February 8-9, 1995.
- Bible, Steven R. and Dan Sakoda. "Petite Amateur Navy Satellite", http://www.sp.nps.navy.mil/papers/ovw_0895.pdf. August 2002.
- Biblarz, Oscar. AA4505 Lecture Notes. Naval Postgraduate School, 2002.
- Carr, Anna, et. al. "Australian CRC for Renewable Energy Ltd.", <http://acre.murdoch.edu.au/refiles/pv/text.html>. July 2002.
- Chase, Charles T. "Annealing of Defect Sites in Radiation Damaged Indium Phosphide Solar Cells Through Laser Illumination", Naval Postgraduate School Thesis, December 1995.
- Clark, Roger N. "Spectroscopy of Rocks and Minerals, and Principles of Spectroscopy", <http://speclab.cr.usgs.gov/PAPERS.refl-mrs/giff/300dpi/fig3a3.gif>. May 2002.
- Department of Energy. "About Photovoltaics", <http://www.eren.doe.gov/pv/gallium.html>. May 2002.
- DeYoung, Robert J. "A NASA High-Power Space-Based Laser Research and Applications Program", 1983.
- Duck, Thomas J. "The Firepond Lidar at Millstone Hill / MIT Haystack Observatory", <http://aolab.phys.dal.ca/~tomduck/milidar/>. August 2001.
- "Electric Propulsion", Aerospace America, December 2001. http://www.aiaa.org/images/01_TC_Highlights/aiaa-ep.pdf.
- Feldhaus, Josef and Rolf Treusch. "FEL Basics", <http://www-hasylab.desy.de/facility/fel/overview/basics.htm>. December 2002.
- Friedman, Herbert W. "Near-Term Feasibility Demonstration of Laser Power Beaming", SPIE Laser Power Beaming Proceedings, January 27-28, 1994.
- Fugate, Robert Q. "Adaptive Optics Techniques for Compensation of Atmospheric Distortions", NASA Goddard Mathematical Tools Seminar, November 7, 1995.
- Fugate, Robert Q. and James F. Riker. "Beam Control for Ground to Space Laser Power Beaming", January 28, 2002.

- Fugate, Robert Q. "Ground-Based Laser Energy Propagation", <http://www.afrlhorizons.com/Briefs/Sept01/DE0108.html>. September 2001.
- Hecht, Jeff. The Laser Guidebook. McGraw-Hill, 1986.
- HELSTF Home Page. <http://helstf-www.wsmr.army.mil/index.htm>. September 2001.
- Hu, Chenming and Richard M. White. Solar Cells: From Basics to Advanced Systems. McGraw-Hill, 1983.
- IFX Fact Sheet. <http://www.sbl.losangeles.af.mil/documents/sblfactsheet.doc>. October 2001.
- Johnson, Robert L., Starfire Optical Range. E-mail conversations, 2002.
- King, D.L., B.R. Hansen, J.M. Moore, and D.J. Aiken. "New Methods for Measuring Performance of Monolithic Multi-Junction Solar Cells", 28th IEEE PVSC, September, 2000.
- Kingsley, Stuart A. "Diffraction Limited Beams and Gaussian Optics", <http://www.coseti.org/radobs14.htm>. January 2002.
- Kuhn, Kelin J. Laser Engineering. Prentice Hall, 1998.
- Landis, Geoffrey A. "Applications for Space Power by Laser Transmission", *OE Reports*, December, 1994.
- Landis, Geoffrey A. "Space Power by Ground-Based Laser Illumination", Intersociety Energy Conversion Engineering Conference, September 15, 1991.
- Landis, Geoffrey A., Mark Stavnes, and Steve Oleson. "Space Transfer with Ground-Based Laser / Electric Propulsion", 28th AIAA Joint Propulsion Conference, July 6-8, 1992.
- Lipinski, R. J. and D. A. McArthur. "FALCON Reactor-Pumped Laser and Applications for Power Beaming to Space", Sandia National Labs Briefing, April 28, 1994.
- Loke, Ching Lan, Robert P. Pfund, and Lori K. Rahko. "Early Communication Using PV Cells", <http://stuweb.ee.mtu.edu/~cloke/EE280/applications.html>. April 2002.
- Mazer, Jeffrey A. Solar Cells: An Introduction to Crystalline Photovoltaic Technology. Kluwer, 1997.
- McCann, Barrett T. Airborne Laser Program Laser Requirements. AA4505 Course Handout, 2002.
- Meriwether, John and Dwight Sipler. "Millstone Hill Lidar", <http://www.haystack.mit.edu/~dps/lidar0.htm>. November 2001.
- Merrigan, Joseph A. Sunlight to Electricity: Prospects for Solar Energy Conversion by Photovoltaics. MIT Press, 1975.
- Michael, Sherif. Personal discussions, Naval Postgraduate School Department of Electrical and Computer Engineering and Space Systems Academic Group.
- Michael, Sherif, Corrine Cypranowski and Bruce Anspaugh. "Forward-Biased Current Annealing of Radiation Degraded Indium Phosphide and Gallium Arsenide Solar Cells", IEEE, 1990.

Monroe, David K. "Laser Power Beaming to Extend Lives of GSO NiCd Satellites", SPIE Laser Power Beaming Proceedings, January 27-28, 1994.

Mucklow, Glenn H. "Electric Propulsion", <http://spacescience.nasa.gov/osstech/epropuls.htm>. August 2001.

National Aeronautics and Space Administration. 2nd NASA Conference on Laser Energy Conversion, January 27-28, 1975.

Nored, Donald L. "Application of High Power Lasers to Space Power and Propulsion", 2nd NASA Conference on Laser Energy Conversion, January 27-28, 1975.

Oleson, Steven R. and John M. Sankovic. "Advanced Hall Electric Propulsion for Future In-Space Transportation", NASA Glenn Research Center, 1999.

O'Gara, Dan. "LURE Observatory's Satellite Laser Ranging (SLR)", <http://koa.ifa.hawaii.edu/Lure/>. September 2002.

O'Shea, Donald C., Callen, and Rhodes. Introduction to Lasers and Their Applications. Addison-Wesley, 1978.

Peat, Chris. "PANSAT – Information, Heavens Above", <http://www.heavens-above.com/satinfo.asp?SatID=25520&lat=36.600&lng=-121.894&alt=23&loc=Monterey&TZ=PST>. September 2002.

Pike, John. "Air Force Maui Optical Station", <http://www.fas.org/spp/military/program/track/amos.htm>. May 2002.

Pike, John. "Mid-Infrared Advanced Chemical Laser", <http://www.fas.org/spp/military/program/asat/miracl.htm>. July 2001.

Pike, John. "Space Based Laser", <http://www.fas.org/spp/starwars/program/sbl.htm>. August 2001.

Preuss, Paul. "Earth to Space: Powering Communication Satellites from the Ground", <http://www.lbl.gov/Science-Articles/Archive/ground-satellite-power.html>. July 2002.

Rauschenbach, H.S. "Solar Cell Array Design Handbook, Volume 1", NASA JPL, October 1976.

Reinhardt, Kitt, Michael Price, and Robert Drerup. "ManTech for Multi-Junction Solar Cells", <http://www.afrlhorizons.com/Briefs/Sept01/ML0007.html>. August 2002.

Sakoda, Dan. "An Overview of the Petite Amateur Navy Satellite (PANSAT)", 13th AIAA/USU Conference on Small Satellites, August 23-26, 1989.

Sakoda, Dan. "PANSAT Home Page", <http://www.sp.nps.navy.mil/pansat/>. August 2002.

SBL FAQ, http://www.sbl.losangeles.af.mil/IFX_FAQ/FAQs.htm. August 2001.

Seale, Eric. "Solar Cells", http://encyclobeamia.solarbotics.net/articles/solar_cell.html. June 2002.

Seale, Eric. "Solar Cells: Shedding a Little Light on Photovoltaics", http://www.solarbotics.net/starting/200202_solar_cells/200202_solar_cell_types.html. June 2002.

Seale, Eric. "The Photovoltaic Effect", <http://encyclobeamia.solarbotics.net/articles/photovoltaic.html>. June 2002.

Siegman, Anthony E. Lasers. University Science Books, 1986.

Skinner, Mark, Boeing Maui Site Support. E-mail conversations, 2002.

Snodgrass, Josh, Capt, USAF. E-mail conversations, 2002.

Spitzer, A. "Near Optimal Transfer Orbit Trajectory Using Electric Propulsion," American Aeronautical Society Paper 95-2515, February 13-16, 1995.

Starfire Optical Range Home Page, <http://www.de.af.mil/SOR/>. January 2002.

Stirn, Richard J. "Photovoltaic Conversion of Laser Energy", 2nd NASA Conference on Laser Energy Conversion, January 27-28, 1975.

Talbot, John P. "Airborne Star Wars Laser", <http://home.achilles.net/~jtalbot/history/starwars.html>. December 2001.

Walters, Donald. PH4251 Class Notes. Naval Postgraduate School, 2002.

Wertz, James R. and Wiley J. Larson. Space Mission Analysis and Design. 3rd edition. Microcosm Press, 1999.

Williams, M.D., J.H. Kwon, G.H. Walker and D.H. Humes. "Diode Laser Satellite Systems for Beamed Power Transmission", NASA Technical Paper 2992, 1990.

WSMR Public Affairs. "High Energy Laser Systems", <http://www.wsmr.army.mil/paopage/Pages/laser.htm>. August 2001.

"Xenon Ion Propulsion". Boeing Public Relations, <http://www.hughespace.com/factsheets/xips/xips.html>. February 2002.

Ziemer, John K. "Laser Ablation Microthruster Technology", 33rd AIAA Plasmadynamics and Lasers Conference, May 20-23, 2002.

INITIAL DISTRIBUTION LIST

1. Defense Technical Information Center
Ft. Belvoir, Virginia
2. Dudley Knox Library
Naval Postgraduate School
Monterey, California
3. Air Force Research Laboratory
Directed Energy Directorate (AFRL/DE)
Kirtland AFB, New Mexico
4. Air Force Research Laboratory
Air Force Maui Optical and Supercomputing Site (AMOS)
Maui, Hawaii
5. National Aeronautics and Space Administration
Marshall Space Flight Center
Huntsville, Alabama